H1-06/04-612
6 July 2004.

Magnetic Monopole Search Status Report

Editors, D. Milstead and T. Sloan.
Referees, E. Elsen and S. Levonian.

Abstract

In the first part of this (written June 2003) we review the analyses of the central beam pipe measured in December 2002 and January 2003 and the data on the downstream beam pipe taken 1 May 2003. In the second part (written Feb 2004) the results of the 15 Jan 2004 run have been added. In this run the measurements on the downstream pipe made in May were redone and the central pipe sections were also remeasured. No signals for magnetic monopoles were observed and upper limits on the production cross section are derived.

First Part - written 18/6/03

1 Introduction

We have had 3 runs on the Southampton 2G magnetometer. In Dec 2002 and Jan 2003 we measured the central beam pipe. In May 2003 we measured the downstream beam pipe and repeated the measurements of the central beam. The analyses of the data from the central beam pipe taken in the Dec and Jan runs has been released in a preliminary form at DIS2003. In this report we review these analyses and present the data (including the downstream beam pipe measurements) taken in the 1 May run.

In the 1 May run we did more extensive calibrations to try to understand the calibration completely. We found that the calibration scale (magnetometer reading per Dirac Monopole) needed to be decreased by 25% for the Dec runs and it needed to be increased by a factor of 2 for the Jan runs. The details of these measurements are described below. We show that the calibration is now completely understood to an accuracy of about $\pm 5\%$. Reanalysis of the Dec-Jan data with the new calibration confirms our preliminary result on the central beam pipe covering the pseudorapidity range $|\eta| < 2.55$. The May data proved to be much more noisy and less clean than the Dec and Jan runs and these measurements are described.

2 The Calibration

2.1 The calibration itself

The calibration was performed by passing coils through the magnetometer and observing the size of the step readings. Four coils have been used and these are described in table 1. Usually the coils are demagnetised (0.1 T at ~ 400 Hz) before passing them through the magnetometer to reduce residual dipole moments.

Table 1: Description of the Calibration Coils used

Coil	1	2	3	4
Core diam.(mm)	6.08	3.15	2.1± 0.1	2.1± 0.1
Wire diam.(mm) (including insulation)	0.18	0.18	0.1	0.1
Bare Wire diam.(mm)	0.15	0.15	0.08	0.08
Turns per metre	11000	11000	10000	30000
Calculated resistance (ohms)	151	81.5	58.4	177
Measured resistance (ohms)	141	78.7	56.0	180
Area (mm^2) (including wire)	32.6	9.7	3.80	4.54
Uncertainty in area	3.3%	6.0%	10%	10%
Dirac monopoles per μA	109.0	32.4	11.6	41.4

To calibrate, the step size from each coil is measured and normalised using the values given in table 1. Fig 1 shows the magnetometer scale reading per Dirac Monopole for all the calibrations made, plotted as a function of the pole strength of the calibration. This pole strength is calculated from the expression

$$g_D = n\ \delta S\ i/3.291\ 10^{-9}\text{Dirac Monopoles} \tag{1}$$

where i is the current in the coil which is wound with n turns per unit length. This simple formula has been checked to be accurate to better than 1% by integrating the field from all elements of the coil using the Biot-Savart expression for the magnetic field due to each element. The effective area, δS, is the most inaccurate part of the calibration. We think the effective diameter of each coil is determined to an accuracy of 0.1 mm which causes a larger uncertainy in the smaller coils than in the larger coils. Table 2 summarises the means and standard deviations of the calibrations from each coil. The spread of the calibrations from the different coils (table 2) in fig. 1 indicates that the coil areas must be well determined. Hence the quoted uncertainties on the coil diameters are probably somewhat overestimated.

Table 2: Means and standard deviations of calibrations from all coils

Coil	1	2	3	4
Mean ($\cdot 10^7$) (Magnetometer current per Dirac Monopole)	1.10	1.09	1.11	1.11
Standard Deviation	0.016	0.024	0.030	0.017
No. of readings	5	18	4	13
Mean calibration	1.10 ± 0.007	1.09 ± 0.006	1.11 ± 0.015	1.11 ± 0.005

2.2 History of the Calibrations

Fig 1 shows good consistency between all the calibrations performed except for one point (coil 3 at close to $g_D = 1$ Dirac Monopole, the last point taken in the Dec run, the rogue point).

In the Dec run only coil 3 was used with 3 calibration points (at 1.2,12 and 88 Dirac monopoles) which were not quite consistent with each other. We decided to use the point for coil 3 at $g_D = 1.2$ Dirac Monopole as our main calibration since this is the closest to our desired range of values. Fig 1 shows that this is the only rogue point in the data. Hence the calibration in the previous analysis of the Dec data was about 25 $\%$ off. The reason for this rogue point could be as follows. The coil power supplies were battery driven. It was found in the January run that the battery used for the Dec run was flat. The rogue point was the last one taken in December hence it is possible that the battery had already deteriorated when we took the data for that point. For this reason we disregard this rogue point and readjust our December calibration to the mean in figure 1 i.e. $1.10\ 10^{-7}$ magnetometer units per Dirac Monopole for the magnetometer output labelled Z_{int}. The calibration from the magnetometer output labelled Z_{corr} is 1.79 times larger than this i.e. $1.97\ 10^{-7}$ units per Dirac Monopole.

When we analysed the Jan run we were forced to use coil 2 and could not cross check with coil 3 since we broke its very thin wire when we tried to use it. Unknown to us at the time is that coil 2 had been wound in two layers (we had requested one) so that it had twice as many turns as we thought. The second layer was hidden by the first. Hence our calibration for the Jan run was out by a factor 2. This was discovered by comparing the calculated and measured resistances of the coils (table 1).

When these problems are corrected figure 1 shows that we have the same calibration in Dec,Jan and May for all coils consistent with our expectation of the high quality 2G apparatus.

3 Results of the Central Beam Pipe Measurements

Fig 2 shows the analysis of all the central beam pipe strips using the calibration of $1.1\ 10^{-7}$ magnetometer units per Dirac Monopole. The first minus the last reading in the data stream is taken and normalised by the calibration as we described in our preliminary paper. It is interesting that our monopole candidates seen in December are now +0.7 Dirac Monopoles rather than the value previously close to 1.0. Strip 3 had one previous measurement with -0.3 Dirac Monopoles which has now moved to -0.7 monopoles with the new calibration. The latter fluctuation disappears if the next to last reading is used instead of the last reading. Hence this fluctuation is probably due to a speck of magnetised dust on the carriage and is ignored.

We had a number of other small samples from the central beam pipe. For example two strips were sawn into multiple small pieces each about 1 cm wide. The saw dust chippings from all cuttings were collected and included with these small samples. Figure 3 shows the analysis of all these small samples from the measurements taken in Jan. Sample 35 (some of the saw dust chippings) showed a fluctuation also at ~ 0.7 Dirac Monopoles in two separate measurements in January i.e. clear monopole behaviour. However, the readings were different on remeasurement in May. Hence this result is not due to a trapped monopole. It was decided to exclude these saw dust chippings since they probably will be contaminated by material with large dipole moments.

In conclusion, in the Dec-Jan measurements we saw 3 large fluctuations in 71 readings none of which repeated on remeasurement. We conclude that such fluctuations (at the level of ~ 0.7 Dirac Monopoles) are not monopoles, unless they are due to monopoles which diffuse out of the pipe before remeasurement. This seems implausible since it is thought that the monopoles will be tightly bound to nuclear dipoles in the Aluminium ([1]). Hence the apparatus must be susceptible to random flux jumps or a failure to restore the base line at the level of ~ 0.7 Dirac Monopoles. Such effects became much more frequent in the May run (see below).

4 Analysis of the Downstream Beam Pipe - 1 May 2003

The downstream beam pipe (covering the range $4.2 > \eta > 2.6$) was cut into 3 sections (pipe 1,2 and 3 downstream from the central beam pipe) and each of the sections divided into 10 strips of width approximately 30 mm. The strips were passed through the magnetometer in much the same way as the readings for the central beam pipe. Figure 4 shows the step sizes ((last reading-first reading)/calibration constant) versus strip number for all the data taken in May.

A somewhat different running procedure was adopted in May. It was felt that, since we were only interested in the final persistent current, it was not necessary to have so many intermediate readings. In general 20 cm step sizes were adopted for the samples (8 readings per sample, although some samples were measured in smaller step sizes and some were measured in 40 cm step sizes) compared to 2-5 cm steps in Dec-Jan. Hence the data taking was much faster in the May run. Two passes were made for each sample. One pass was taken passing the +z end of the strip through first (i.e. the downstream or proton end of the strip) and the second run passing the -z end (upstream or electron) through first. In fig. 4 the open circles are the readings with the -z ends first and the closed circles with the +z end first. It can be seen that when we passed the +z end first the data scatter roughly about zero but when we passed the -z end first the data scatter about -0.7 Dirac Monopoles. Some of the measurements with +z first scatter about +0.7 Dirac monopoles. This was an effect of time. The ones scattering about +0.7 were among the first runs taken but those scattering about zero came later. This can be seen in fig 5 where the normalised step sizes are plotted against run number (i.e. time). In the first 14 runs the +z passes all measured $\sim +0.7$ Dirac Monopoles and after this the readings scatter around zero.

There is clearly a pattern to the observed fluctuations in figures 4 and 5. This can be seen from figure 6 which is similar for all runs. The readings for the +z(-z) end passing first give dipole background moments which are always strongly positive (negative) and these induce positive (negative) final currents. What is difficult to understand is why the Dec and Jan runs gave stable base lines with only 3 large fluctuations in 71 readings while in the May run we saw frequent fluctuations (all runs with -z first gave a negative fluctuation) which are correlated with the sign of the dipole background.

How do we interpret the data in figure 4 ? It is difficult to understand these data. However, if a monopole had been trapped in one of the samples both the +z and -z readings would be displaced from their usual values for that sample. This is not observed. Hence one concludes that there is no evidence of a signal from a monopole of strength 1 Dirac Monopole or greater present in the measurements taken in May.

What do we do in this situation ? What are our alternatives ?

- We could return to Southampton and repeat the May measurements. Ugh - 3 days in Southampton -what a thrilling prospect !
- We could abandon the downstream pipe which will lose us the high mass region.
- We could apply a shift of +0.7 Dirac Monopoles to all the -z runs and similarly a shift of -0.7 Dirac Monopoles to all of runs 2040-2070 ??

Second Part - written 8/3/04

5 Analysis of the Downstream Beam Pipe - Data taken 15 Jan 2004.

The decision to do another run on the downstream beam pipe sections was made and the run took place on 15/1/04.

5.1 The Calibration

The calibration was made in the usual way using coil 2. Figure 7 shows all the calibrations again as in figure 1 (open points) together with the new calibration points superimposed (solid black squares). The solid black squares show the output $Bz_{intensity}$ per Dirac Monopole for the data taken on 15 Jan 2004 as a function of the pole strength of the long coil. These calibrations tend to scatter more widely than those in figure 1 with a mean of 1.085 units per Dirac Monopole and a standard deviation of 0.083 (excluding the points at $g_D = 0.27$). The lowest points at $g_D = 0.27$ had some residual contamination at both the beginning and end of the scan (see figure 8). This reduced the calibration step taken from the difference of the means of the first 4 and the last six readings. The probable reason for the larger scatter than in previous runs (see table 2) is that we forgot to demagnetise coil 2 in the January 2004 run. This left larger residual dipole moments in the coil material and hence more noise in the system (see below).

The calibration in the Jan 2004 run is compatible with the value $1.10\ 10^{-7}$ units per Dirac Monopole found in the Dec, Jan and May runs (see table 2) and this figure will be used throughout this analysis.

5.2 A possible explanation of the May data on the downstream beam pipe.

The strips were found to retain a fixed dipole strength. This is illustrated in figure 9 which shows the dipole strength as a function of the z position of the measurement for a single strip passed through with it pointing along the proton beam direction ($+z$ first) and when it was reversed ($-z$ first). The readings at small z in figure 9 correspond to the most downstream point on the strip. It can be seen that the dipole strengths with $-z$ first are an inverted mirror image of those with $+z$ first showing that the permanent dipole moments reverse sign on reversing the strip direction. It is interesting that the more downstream the position of the measurement, the stronger the permanent dipole moment.

Figure 10 shows the relative dipole strength of several of the aluminium strips superimposed on the same plot, all passed $+z$ first, as a function of position in the beam pipe . A schematic diagram of the beam pipe showing the sections into which it was cut is superimposed in the lower section of the plot. The H1 magnetic field is in the $+z$ direction. All the strips are found to be magnetised in the same way (positive dipole moment) with similar dipole strengths.

Hence the aluminium became permanently magnetised in the direction of the H1 field direction at a level of $\sim\ 10^{-3}$ of the induced dipole moment per unit volume expected from the H1 magnetic field (21 Am^{-1} = 0.021 em per cm^3). The dipole strength increases with z and seems to be higher in the downstream sections (pipes 2 and 3, the dipole moments for pipe 1 are not available) than in the central region. This could be due to the contamination of the downstream pipe due to evaporation from the collimator C4 during beam tuning.

There was some evidence that the 2G's ability to restore its base line depends on the strength of the dipole moment which has passed through. This can be seen by comparing figures 2 and 3 which show the central beam pipe residual currents and those from the small samples. The latter should have the smaller dipole moments and figure 3 shows a smaller scatter of the points than figure 2 (except for sample 35 - we did not measure the dipole moment of this sample since we only measured the original and final 2G readings). Perhaps for dipole strengths above a critical level the machine has difficulty restoring its base line. Such a critical level could be passed for the downstream sections but not by the strips from the central beam pipe. This would explain the jumps to -0.7 Dirac Monopole Unit seen when measuring the downstream sections of pipe tested in the May run. However, why does the current jump to -0.7 Dirac Monopole Units (equivalent to $7.7\ 10^{-8}$ emu per cm^3) ? Why is it more prone to such a jump for negative dipole moments passing than for positive ? We need to discuss with the experts.

5.3 Would we have seen a Monopole in the May Run ?

In order to test that we would have seen a monopole in the May run we positioned the calibration coil throat (coil number 2) at the centre of a sample (pipe 3 strips 9 and 10, paired so that the +z of one is opposite the -z of the other). The strip was then passed through in the normal way with different currents flowing in the coil. Before positioning the coil on the sample it was checked that it showed the behaviour seen in the May run (see figure 11).

Unfortunately for this test we made two mistakes.

- We forgot to demagnetise the calibration coil (coil 2) which had a substantial dipole moment. We did this in the previous runs allowing us to produce the step plot shown in the paper sent to last summer's conferences. Hence a correction for the coil magnetisation is necessary and this was measured from the data.
- We forgot to take a run with zero current in the coil for one orientation (-z first). In addition, the run with $g_D = -1.07$ Dirac Monopole Units and $+z$ first suffered a large flux jump and was unusable.

The coil magnetisation was measured and corrected for by taking runs with the strip and no coil and subtracting these data from runs with the strip and coil with no current flowing. Runs 3114 and 3115 (reversed direction) have only the strip (pipe 3 numbers 9 and 10 paired) without the coil. We subtract the data of run 3115 from those of run 3123 (coil with zero current) to obtain the coil magnetisation for the +z runs. The data of run 3114 are subtracted from those of the average of the +1.07 and -1.07 Dirac Monopole unit runs (3118 and 3119) to give a measure of the coil dipole moment for the -z first orientation. (We forgot to do a zero current run with the -z first orientation). The coil magnetisation for $z > 0.9$ m, where the correction is crucial to obtain the final persistent current reading, is shown in figure 12. The results were too noisy to be meaningful in the region $z < 0.9$m where the strip dipoles are very large. The two measurements for $z > 0.9$ m agree reasonably well with each other but there are differences at the level of 1 Dirac Monopole unit. Presumably this is Andrew's viscous dipole moments. The data taken with the coil mounted on pipe 3 strips 9 and 10 have the measured coil magnetisation subtracted using the values from runs 3123 - 3115 (open points in figure 12) to correct the +z first data (runs 3121 to 3124) and the data from runs (3118+3119)/2 -3114 (closed points in figure 12) to correct the -z first data (runs 3117 to 3120). All data were corrected for the empty tray run 3116.

Figure 13 shows the results of the measurements on this strip (pipe 3 numbers 9 and 10) taken with coil 2, corrected as described above. Clear steps can be seen superimposed on a shift of -0.7 Dirac Monopoles for -z end first and no shift +z end first. This is illustrated in figure 14 which show the observed step size (mean of last 3 readings) as a function of the current in the calibration coil in Dirac Monopole Units. Figure 15 shows the results of the May measurements in figure 4 together with the data from pipe 3 paired strips 9 and 10 plotted as samples 55, 60 and 65 with a current in the coil equivalent to +1 Dirac Monopole Unit, -1 Dirac Monopole Unit and no coil, respectively. This plot shows that if a monopole had been present in one of the samples it would have shifted both the +z first and the -z first readings by a fixed amount. Hence had a monopole been present in the May measurements it would have been seen as a diplacement of both the +z first and - z first measurements.

We conclude therefore that, had there been a monopole in one of the strips, we would have seen it in the May run since it would have been superimposed on the observed base line shifts of -0.7 Dirac Monopoles with the $-z$ end first and zero with the $+z$ end first.

5.4 Analysis of the Data from the Strips

In the first samples passed through in the Jan 2004 run we saw the same behaviour as in the May 2003 run i.e. no residual step when most of the samples were passed through with the +z direction first but a step at the level of -0.7 Dirac Monopole Units when the sample is passed with -z first. This is shown in figure 16 for one of the strips passed (same one as in figure 9) with the scales enlarged so that the initial and final magnetometer currents can be seen. Similar behaviour was observed for all the 9 strips belonging to pipe 3.

Since it is suspected that the failure to restore the base line is due to the passage of a large dipole moment an effort was made to reduce this by passing the strips through in pairs with the pairs oppositely aligned. It was hoped that the negative dipole moment in one alignment would cancel the positive in the other. However, the problem observed in May still persisted on a significant fraction of the strips tried (on 3 attempts there was no residual step for the -z direction first traversal but on 5 attempts there was a step). The reason is probably that the dipole moments only partially cancel when the strips are oriented in this way (see figure 11).

Finally it was decide to demagnetise the samples. Monopoles at the level of strength of the order of 1 Dirac Monopole Unit are thought to be very tightly bound in Aluminium with binding energies of the order of 1 MeV [2]. Hence a demagnetising field of 0.1 T (only 1/10 of the H1 field) should not dislodge a monopole. Figure 17 shows that demagnetisation reduces the dipole moments by roughly a factor of 20.

All the strips were passed through again but demagnetising before taking the readings. Figure 18 shows the residual magnetometer current steps versus sample number. Sample 17 is 13 (out of 15 total) strips of the central beam pipe taped into one section and passed through. There is no evidence for a monopole in any of the samples measured i.e. in the whole of the beam pipe (including the small samples, figure 3). Table 3 lists the strips corresponding to each sample number in figure 18.

Table 3: List of sample numbers in Figure 18. The samples generally were placed with the $+z$ end of one opposite the $-z$ end of the other. The central beam pipe sample had all pointing in the $+z$ direction when known. All samples in figure 18 were demagnetised.

Sample	Description.
1	Half pipe 1 strip 3, Half pipe 1 str 5 and pipe 1 str 6 (both halves).
2	Pipe 1 str 8 (both halves) and pipe 1 str 10 (both halves)
3	Pipe 1str 7 (both halves), pipe 1 str 4 (both halves)
4	Other half pipe 1 str 3, other half of pipe 1 str 5 and pipe 1 str 9 (both halves)
5	Pipe 1 str 2 (both halves), pipe 1 str 1 (both halves)
6	Pipe 2 str 1 and pipe 2 str 2
7	Pipe 2 str 3 and pipe 2 str 4
8	Pipe 2 str 5 and pipe 2 str 9
9	Pipe 2 str 6 and pipe 2 str 8
10	Pipe 2 str 7 and pipe 3 str 8
11	Pipe 2 strip 10 and pipe 3 strip 4
12	Pipe 3 str 1 and pipe 3 str 3
13	Pipe 3 str 2 and pipe 3 str 7
14	Pipe 3 str 5 and pipe 3 str 6
15	Pipe 3 str 8
16	Pipe 3 str 9 and pipe 3 str 10
17	All 13 strips of central beam pipe taped together.

6 Acceptances and Cross Section Limits - written 8/6/04

6.1 Beam Pipe Search

The accptance for monopole detection needs to be known in order to derive limits on the cross section for monopole production. A model of the production process is required to compute this acceptance. All models depend on perturbation theory and in this case the coupling constant is very large invalidating the use of such calculations. Hence all models will be wrong. Nevertheless we press on ignoring this fact and two models were made to determine the acceptance.

Each model assumed that monopoles would be created in pairs with oppositely signed magnetic charge i.e. a North and a South seeking pole is produced in each event. The basis of the models is as follows.

- Model 1 - based on a photon-photon fusion model as shown in figure 19(a). Here the monopoles were assumed to be fermions with spin 1/2. The programme used to generate events was based on one used to generate charm production in DIS and photoproduction by leading order photon-gluon fusion, a photon propagator replacing that for the gluon.
- Model 2 - based on a photon-photon contact interaction as shown in figure 19(b). Here the monopoles were assumed to be bosons with spin 0. Events were generated using the programme CompHEP [3].

In each model the monopoles of a fixed mass were produced and tracked through the H1 magnetic field until they reached the beam pipe. The path length of the monopole in the aluminium beam pipe was then calculated. If this was greater than the calculated range of the monopole in aluminium the monopole was assumed to stop and therefore be accepted. The range of monopoles in aluminium was computed by integrating the stopping power dE/dx given in [4], adjusted for the electron density in aluminium. Fig 20 shows the calculated range (normalised to mass) for monopoles of strength 1 Dirac Monopole Unit versus $p/m = \beta\gamma$ where p and m are the momentum and mass of the monopole, respectively, and β, γ are its velocity factors. The stopping power was computed in [4] by classically considering the long range monopole interactions with atomic electrons. The stopping power increases as the square of the magnetic charge.

The acceptances from each model are shown in figures 21 and 22. The range in the aluminium beam pipe decreases strongly with the magnetic charge on the monopole. Hence the fraction of monopoles which stop (i.e. the acceptance) increases strongly with magnetic charge. The acceptance for South seeking poles is slightly greater than that for North seeking poles since South poles are slowed by the magnetic field allowing a greater fraction to stop in the beam pipe. The acceptance tends to be larger for the $\gamma - \gamma$ fusion model than that for the contact interaction model. This can be understood from the fact that the tranverse momenta of the monopoles tend to be smaller for $\gamma - \gamma$ fusion than for the contact interaction model. This is illustrated in figure 23, which shows the mean value of the tranvserse momentum, p_t, of the monopoles versus monopole mass for the two models. The lower values of p_t for the $\gamma - \gamma$ fusion model leads to more stopping monopoles than the higher values in the bosonic model.

The cross section limits were derived using the smallest of the acceptances in figure 22 (i.e. for N poles in the contact interaction model) to take the most conservative approach. No monopoles were seen i.e. we can say with 95% confidence level that we had less than 3 monopoles trapped in the beam pipe. Hence the upper limit at 95% confidence level on the cross section for monopole production is $3/\mathcal{L}\epsilon$, where $\mathcal{L}$ = 60 pb^{-1} is the luminosity and ϵ is the acceptance. Figure 25 shows the resulting limits on the monopole production cross section as a function of the monopole mass.

6.2 Search in CJC

At the same time as the search for exotic heavily ionising particles and the measurement of anti-deuteron production [5], the data were used to search for tracks which are candidates for magnetic monopoles. Such tracks with dE/dx of more than 10000 MIPs would saturate the CJC electronics. Hence two equal amplitude saturated pulses would have been detected for both z readings of the drift chamber sense wire. The charge sharing algorithm would therefore think that each hit was at the centre of the drift wire, i.e. at z=0. Hence a monopole would appear as an apparent straight track at $\theta = 90$ degrees which had $dE/dx >> 30$ MIPs, the saturation level of the electronics. No such tracks were observed in the minimum bias run of luminosity 5.53 pb^{-1}.

It is not clear that the H1 software or the amplification system would allow such unusual tracks to be written to tape. Let us for the moment ignore these doubts and examine the possible improvements to the cross section limits using a CJC search. The bosonic Monte Carlo was used to determine the acceptances for the search in the minimum bias data i.e. $|\eta| < 1.0$. Monopoles were accepted if they lay in the range $|\eta| < 1.0$ and they did not stop in the beam pipe. Figure 26 shows the limits ($= 3/\mathcal{L}\epsilon_{\mathcal{CJC}}$) on the monopole cross section obtained.

It can be seen from figure 26 that the CJC acceptance is very good for low magnetic charges ($g_D < 1$) since only a small fraction of tracks with such low charge stops in the beam pipe. However, higher magnetic charges mainly stop in the beam pipe and hence have a low efficiency to be detected in the CJC.

The improvement from using the CJC is marginal even for $g_D = 1$ Dirac Monopole unit unless a search could be made over a much higher luminosity. Hence to produce a significantly impoved cross section limit, use of the CJC becomes a major project and we propose at this time to limit the search to the data from the beam pipe alone.

7 Conclusions

H1 does not see magnetic monopoles lodged in its beam pipe, covering $-0.3 < z < 2.0$ m, used in 1996 and 1997. Limits on the electroproduction cross section have been set.

References

[1] K.Milton, G.R.Kalbfleisch, W. Luo and L. Gamberg arXiv:hep-ph/0111062 (see Table 1 of this paper).

[2] References for monopole binding energy.

[3] CompHEP - A.Pukhov et al., arViv:hep-ph/9908288.

[4] S.P. Ahlen, Phys.Rev. **D17** (1978) 229.

[5] H1 Collaboration, DESY 04-032, arXiv:hep-ex/0403056.

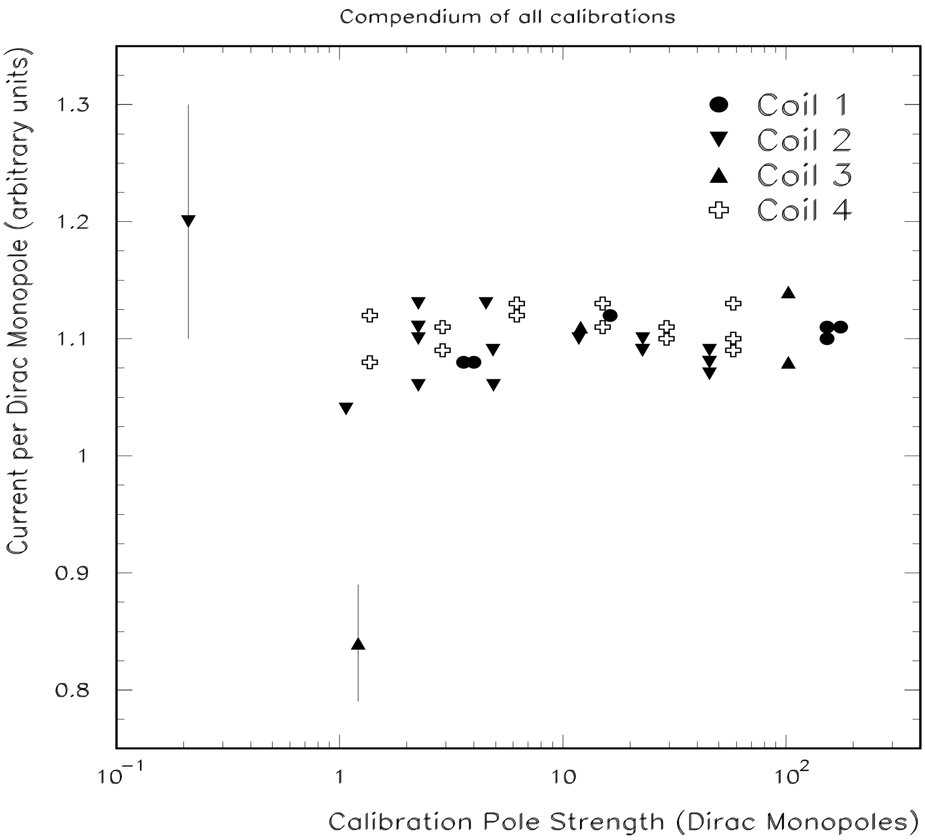

Figure 1: A compendium of all calibrations excluding the January 2004 run (the vertical scale should be multiplied by $1\ 10^{-7}$). In the Dec 2002 run only coil 3 was used (3 calibration points). In the Jan 2003 run coil 2 and one run with coil 3 were used (11 calibration points). (We broke the 0.1mm diameter lead wire after 1 pass of coil 3). In the May run coils 1,2 and 4 were used (26 calibration points).

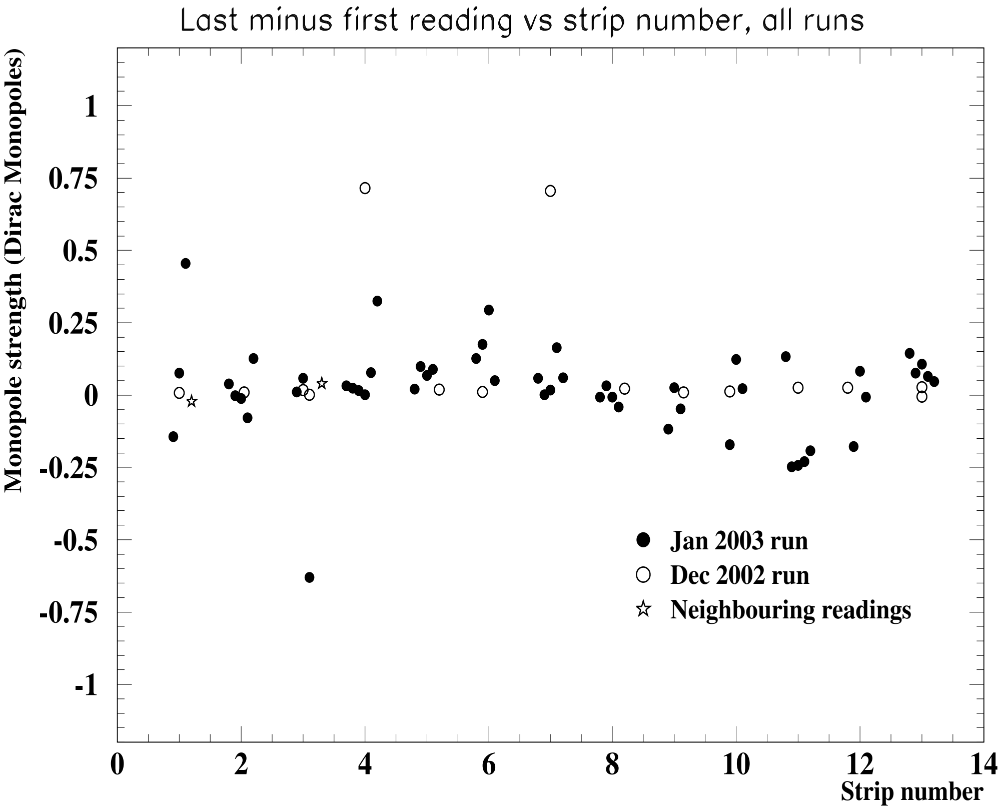

Figure 2: Analysis of all the strips of the central beam pipe using the calibration described in fig 1.

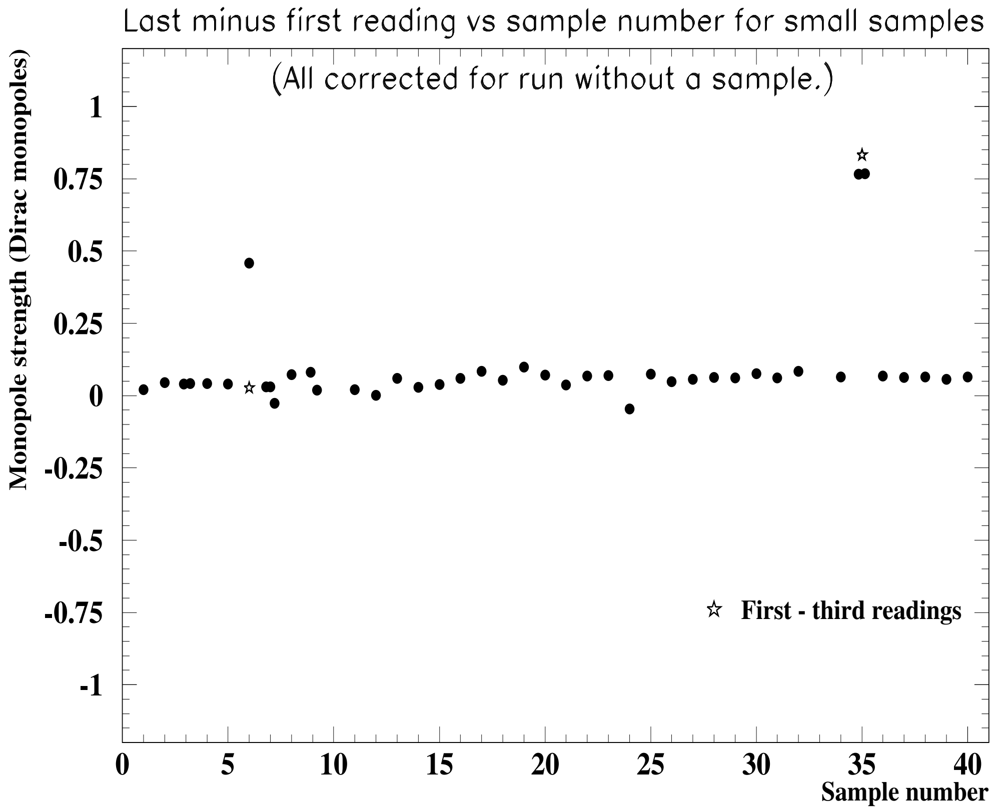

Figure 3: Analysis of all the small samples from the central beam pipe using the calibration described in fig 1. Sample 35 comprised of sawdust chippings and the fluctuation was present on 2 separate runs as indicated.

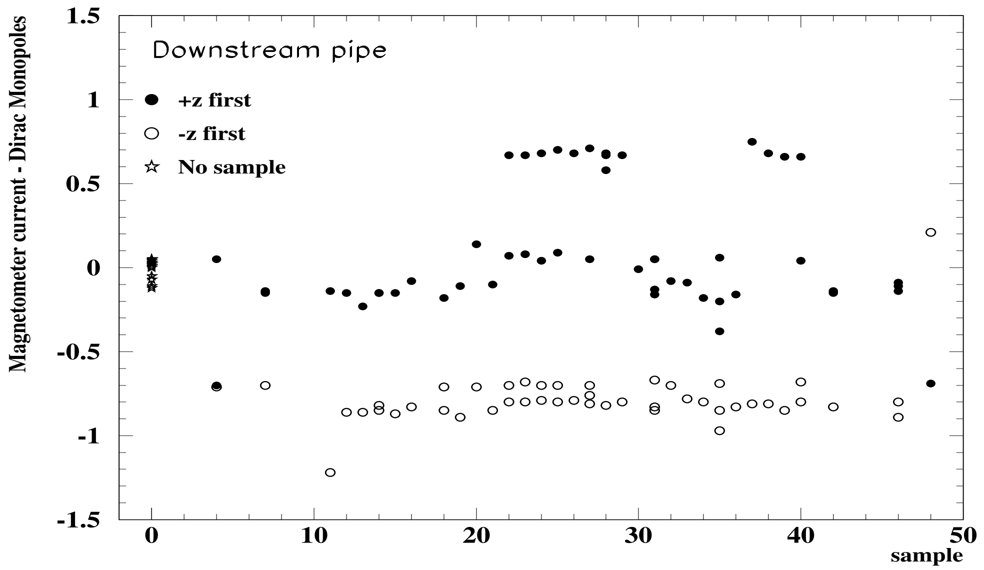

Figure 4: The results of the 1 May run. Samples 11-40 are from the downstream beam pipe. The first digit of the sample number represents the pipe number and the second digit the strip number in the piece of pipe e.g sample 40 means pipe 3 strip 10. The points at sample zero are empty carriage samples (no strip). Sample 42 is strips 31 and 35 combined. Sample 46 is a single small sample from the central beam pipe. Sample 48 is all the small samples, randomly oriented, from the central beam pipe on the carriage at one pass . Sample 7 is strip 7 of the central beam pipe. Sample 4 is the remaining strips of the central beam pipe sent through the magnetometer at one pass.

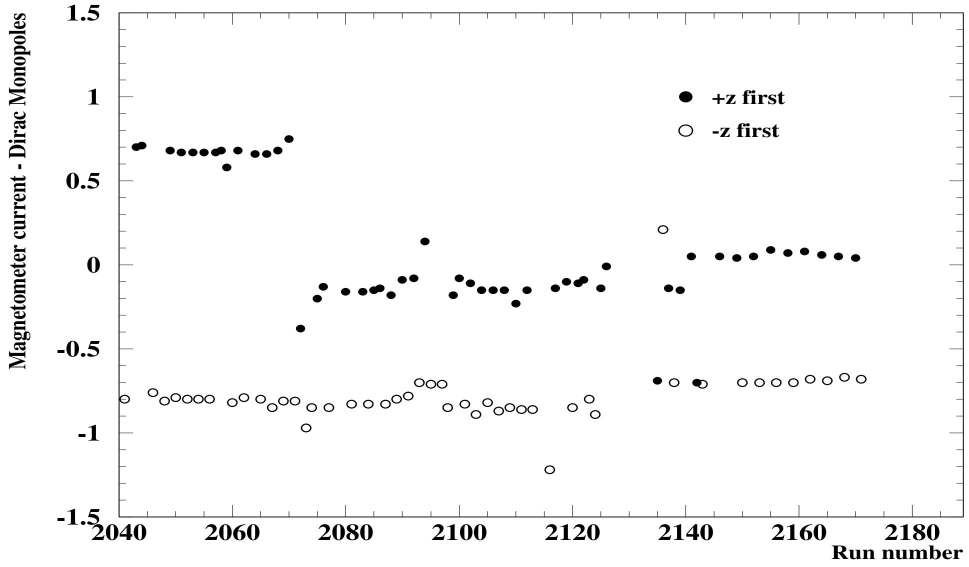

Figure 5: The data in fig 4 plotted as a function of run number (i.e. time).

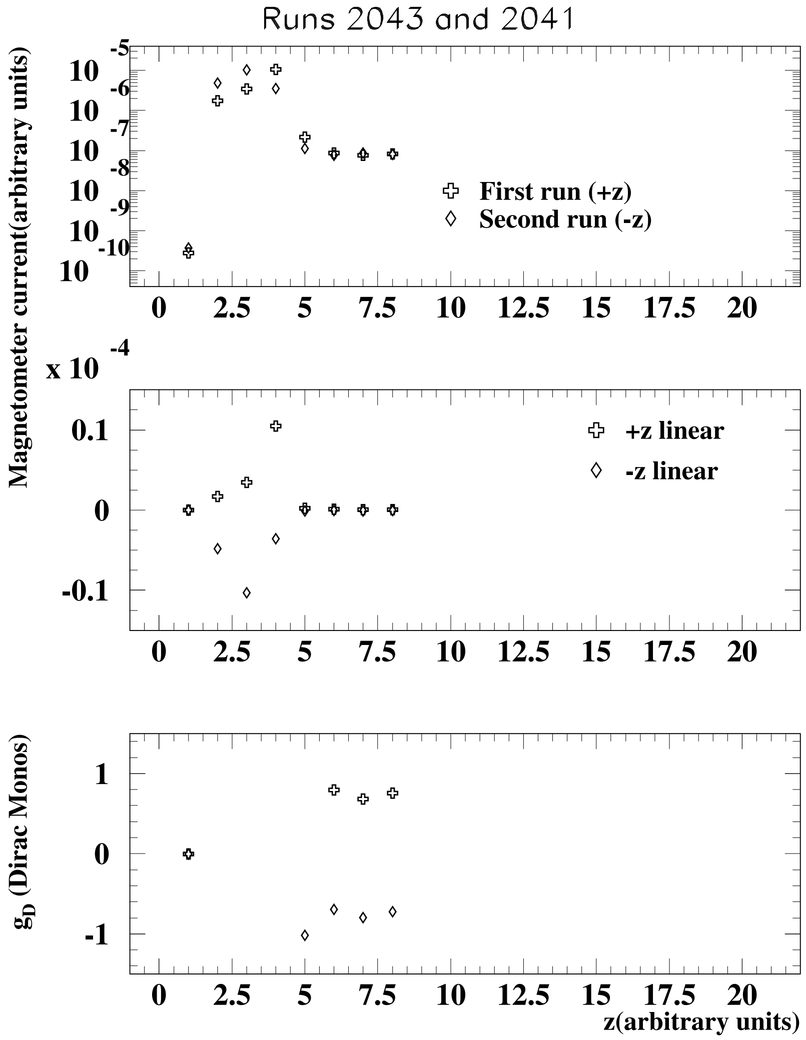

Figure 6: The readings from runs 2041 (-z first) and 2043 (+z first) as a function of longitudinal position. Top shows the absolute readings on a log scale. The middle plot shows the readings on a linear scale and the lower plot the readings on an enlarged linear scale to illustrate the initial and final currents.

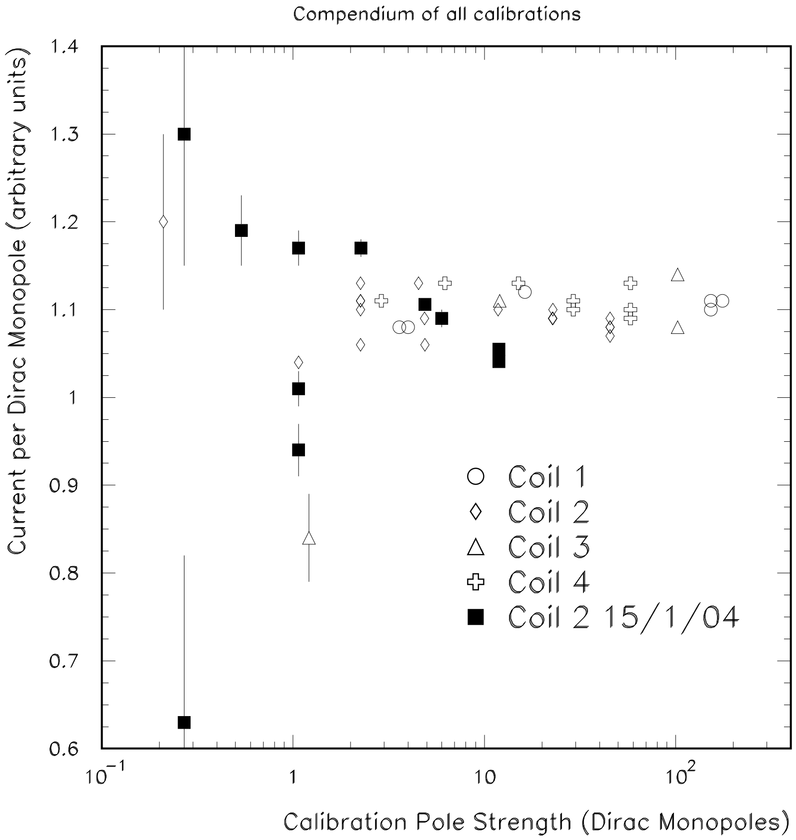

Figure 7: All the calibrations taken in earlier runs (open points from figure 1) together with the calibrations taken in the 15 Jan run (solid squares).NB we forgot to demagnetise the coil for the 15 Jan 2004 run.

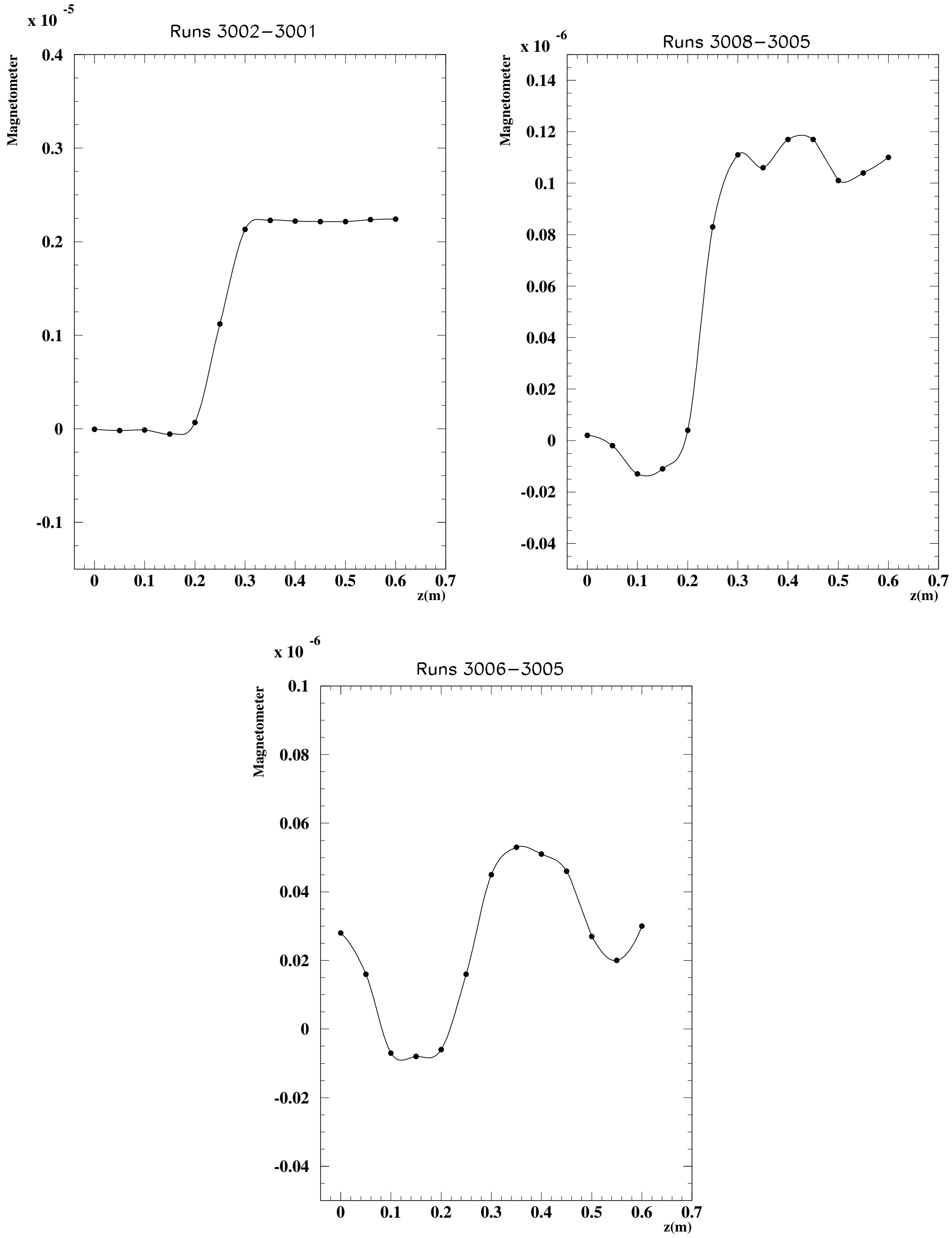

Figure 8: Calibration steps after subtracting a zero current run. Top left shows the step for $g_D = 11.9$, top right for $g_D = 0.538$ and lower plot for $g_D = 0.27$ Dirac Monopole Units. The interfering noise can be seen at the start and finish of the latter. This noise increases the average of the first 3 points and decreases that of the last 4 causing a low calibration value (see figure 7).

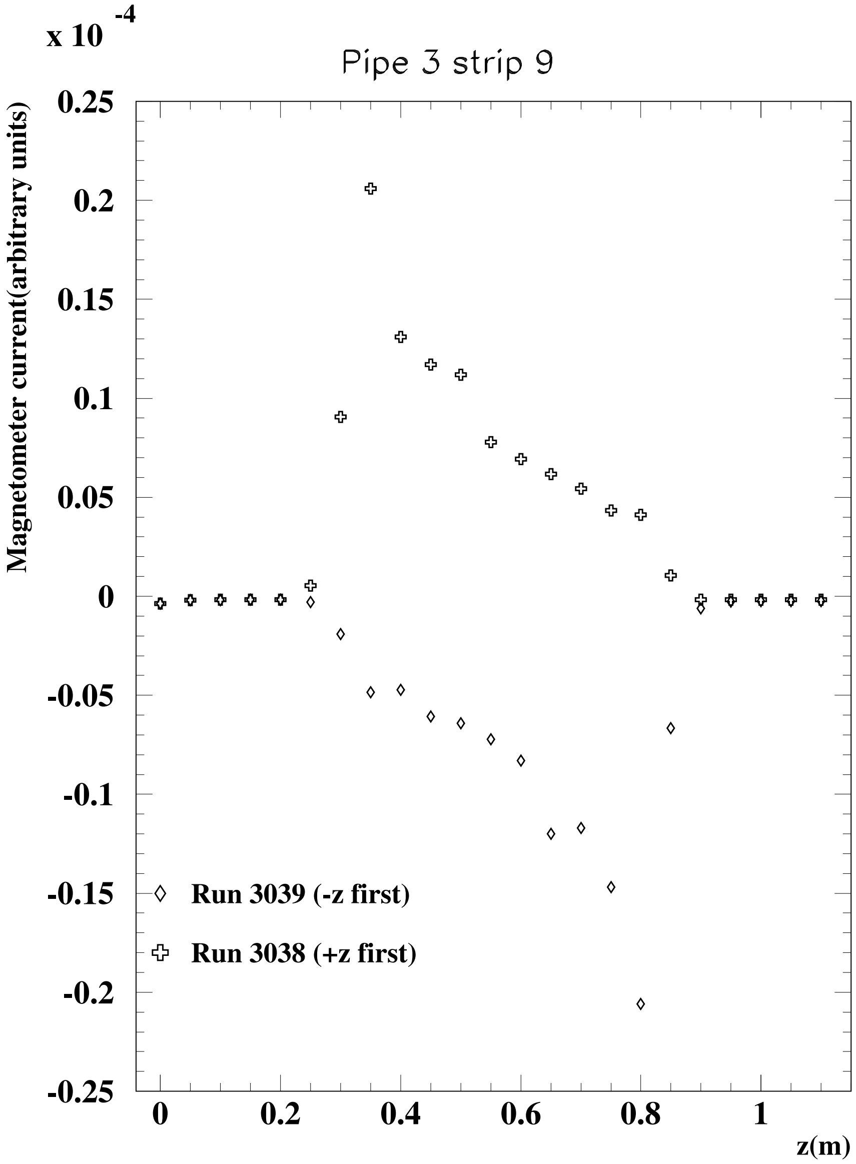

Figure 9: The relative dipole strength as a function of position in the beam pipe (z) along a single strip of pipe 3 first with the strip pointing in the proton beam direction ($+z$ first) and then oppositely ($-z$ first). The vertical axis is the intensity of magnetisation in emu per cm^3 within a factor of 2. (I make it that 1 emu per cm^3 is 1000 Amp m^{-1}). Notice that the dipole moment for one direction of traverse is an inverted mirror image of the other since the dipole moments change direction as the strip is reversed on the traversing tray.

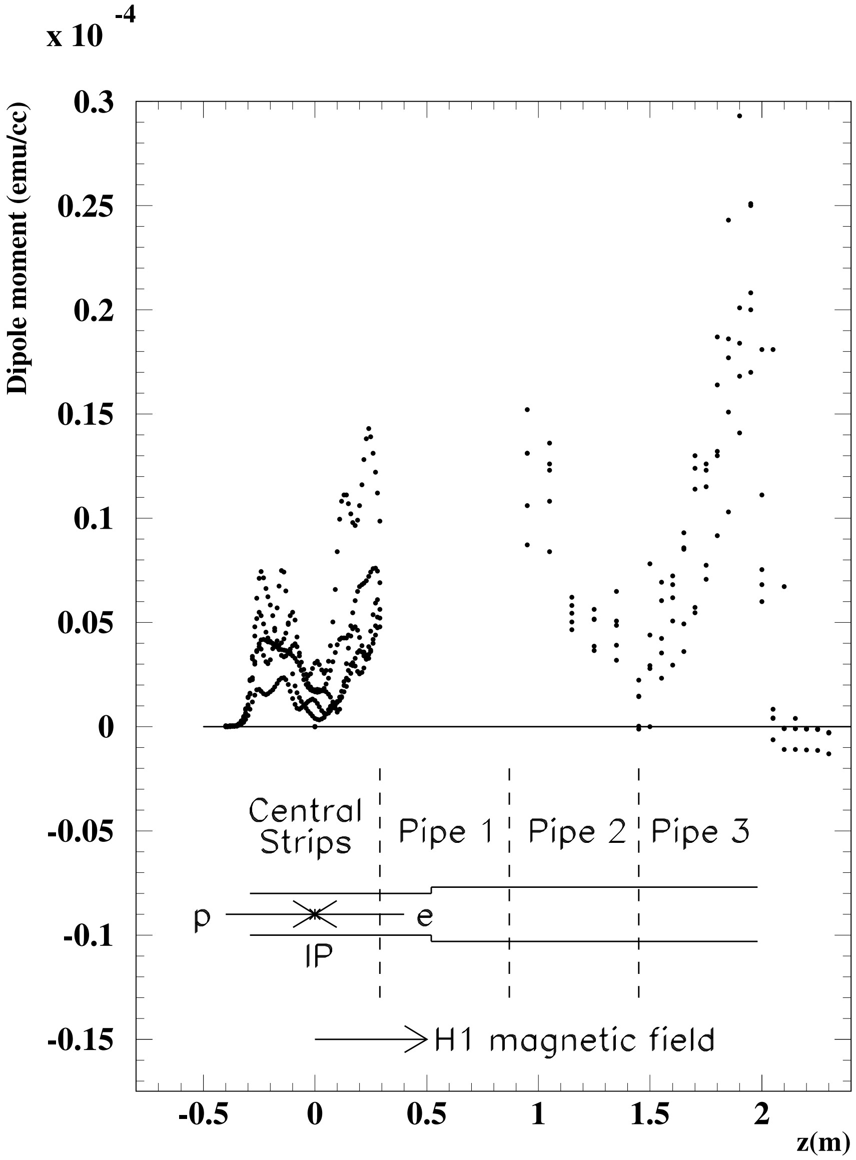

Figure 10: The relative dipole strength as a function of position in the beam pipe (z) for several strips superimposed (all passed with +z first). The different pipe sections measured are shown in the lower schematic diagram. Pipe 1 broke at the weld during cutting and flattening and the two halves were folded together and passed through the 2G. Hence it is difficult to extract the dipole strength vs z for these. The vertical axis is roughly the dipole magnetisation intensity in emu per cm^3 (within a factor of 2).

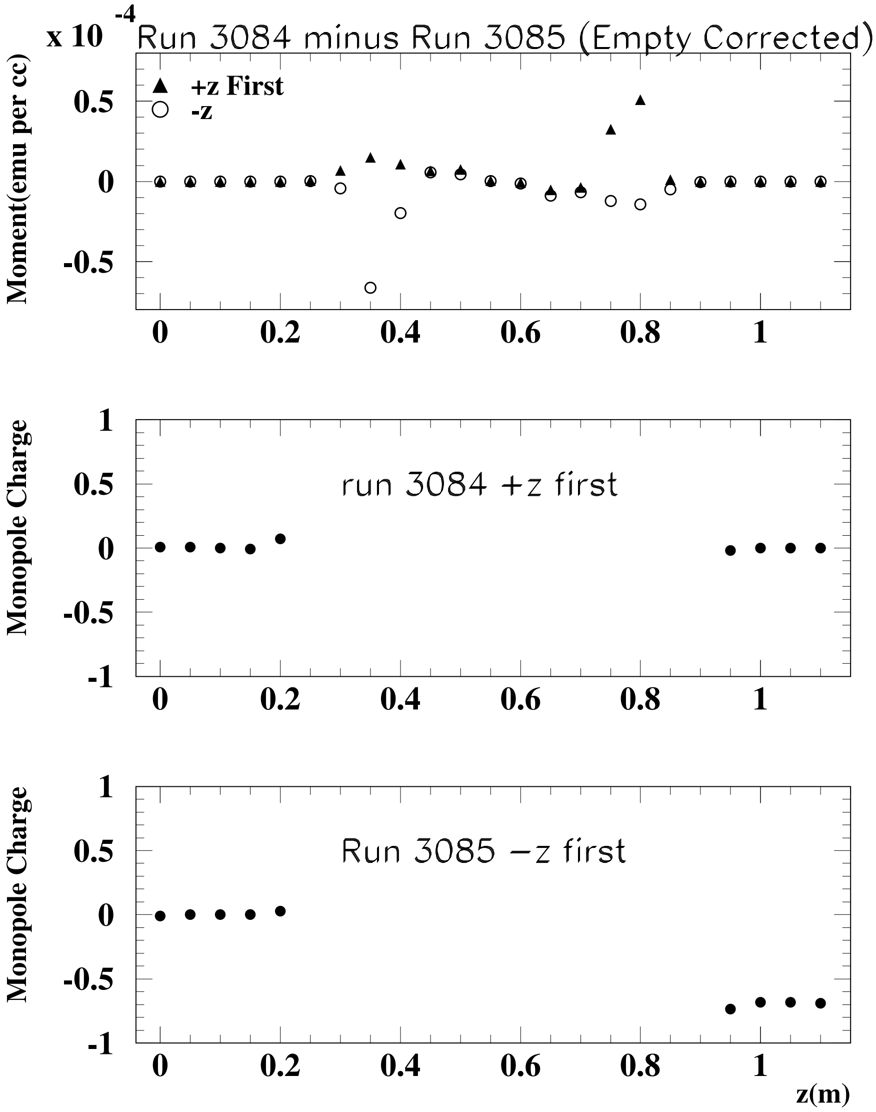

Figure 11: Upper plot shows the measured values of $Bz_{intensity}$ as a function of z as a strip is passed through in opposite directions (no coil superposed on the strip). The strip is the pair pipe 3 numbers 9 and 10 with the $+z$ end of 9 opposite the $-z$ end of 10. The large spike at one end was unique to strip 10 and is untypical (see figures 9 and 10). The middle (lower) plot shows the values of $Bz_{intensity}$ vs z on a larger scale as the strip is passed through in the +z (-z) direction. It can be seen that there is no step for the +z first traversal and a -0.7 Dirac Monopole Units for the -z first traversal i.e. the same behaviour as the May run.

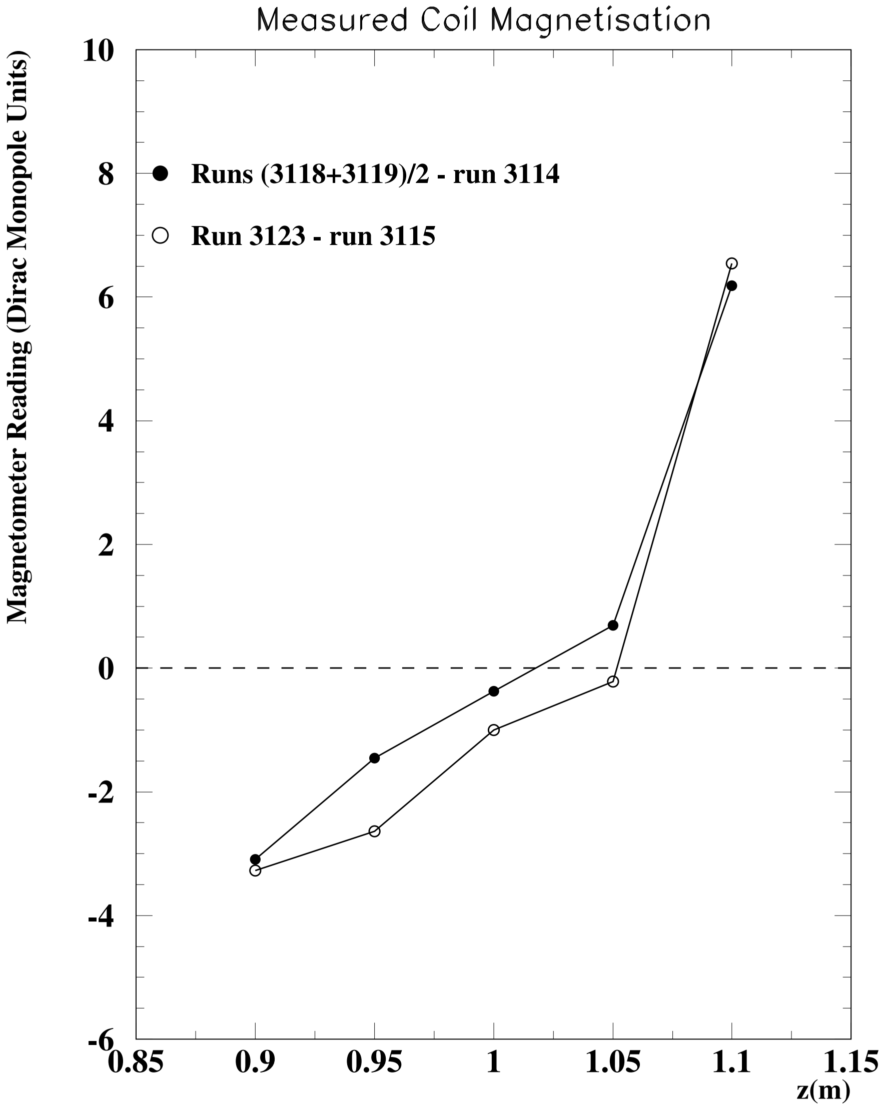

Figure 12: The two measurements of the magnetisation of the coil in Dirac Monopole units. Multiplying the y axis by 1.10e-7 gives approximately the magnetisation of the copper of the coil in emu per cc.

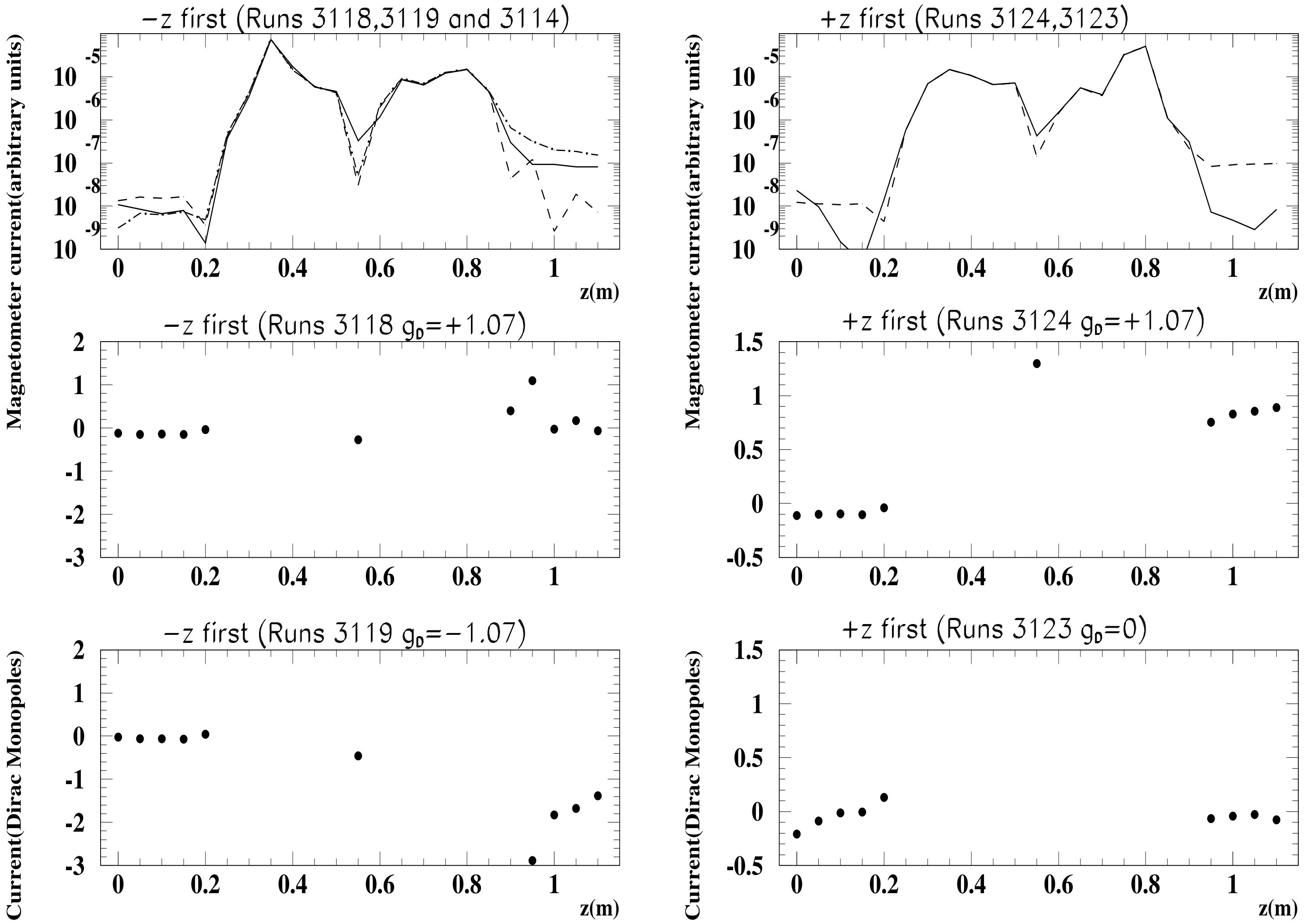

Figure 13: The measurements of pipe 3 strips 9 and 10 paired in opposition with coil 2 superposed after corrections for empty tray and the coil dipole moments (see text). The upper plots show absolute magnitudes on a log scale for +1.07 (dashed), -1.07 (dash dotted, data lost due to large flux jump on right hand plots) and zero (solid curves) Dirac Monopole Units. The left hand plots show the results when the -z end passes first and the right hand plots when the +z end passes first. The linear scale plots show the data with currents of +1.07 and -1.07 Dirac Monopoles for -z end first and +1.07 and zero for +z first (we lost the -1.07 run due to a large flux jump). The steps are seen superimposed on a -0.7 Dirac Monopole jump in the left hand plots and no jump in the right hand plot i.e. the May run behaviour.

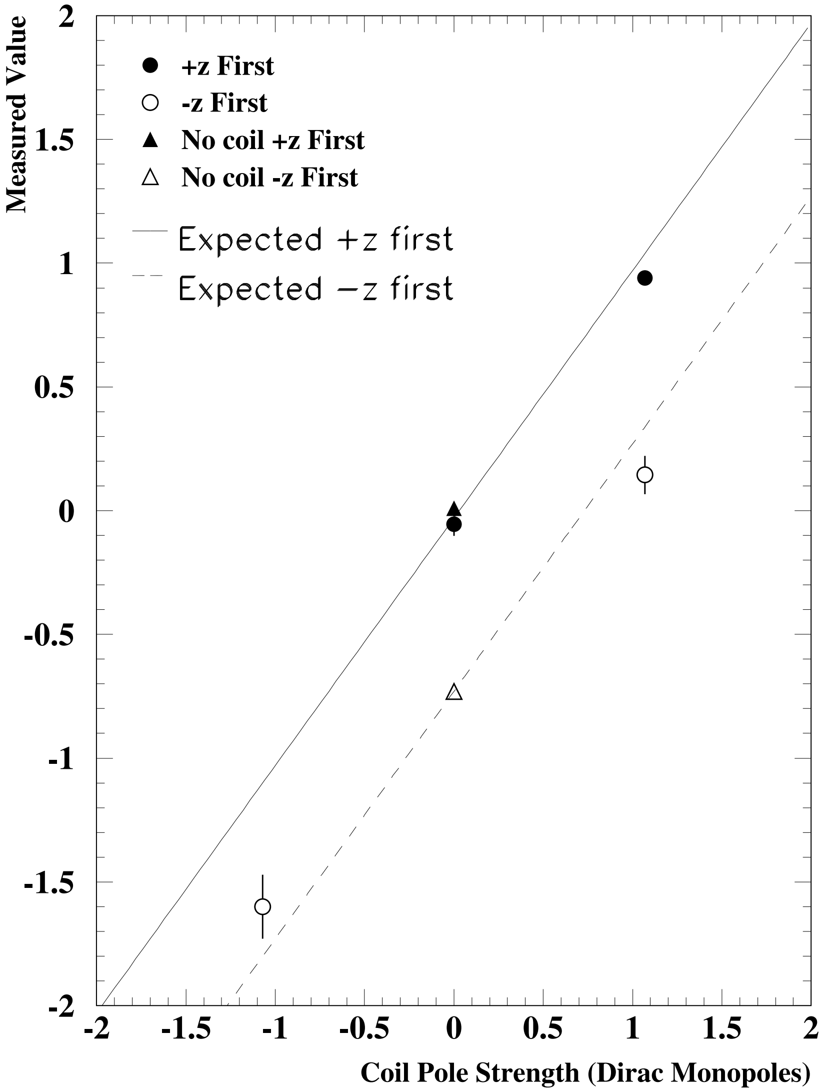

Figure 14: The observed step sizes versus the coil excitation current in Dirac Monopole Units. The solid line shows the expected behaviour for no base line shift when the $+z$ end is passed through first and the dashed line that with a jump of -0.7 Dirac Monopole units as the $-z$ end is passed through first.

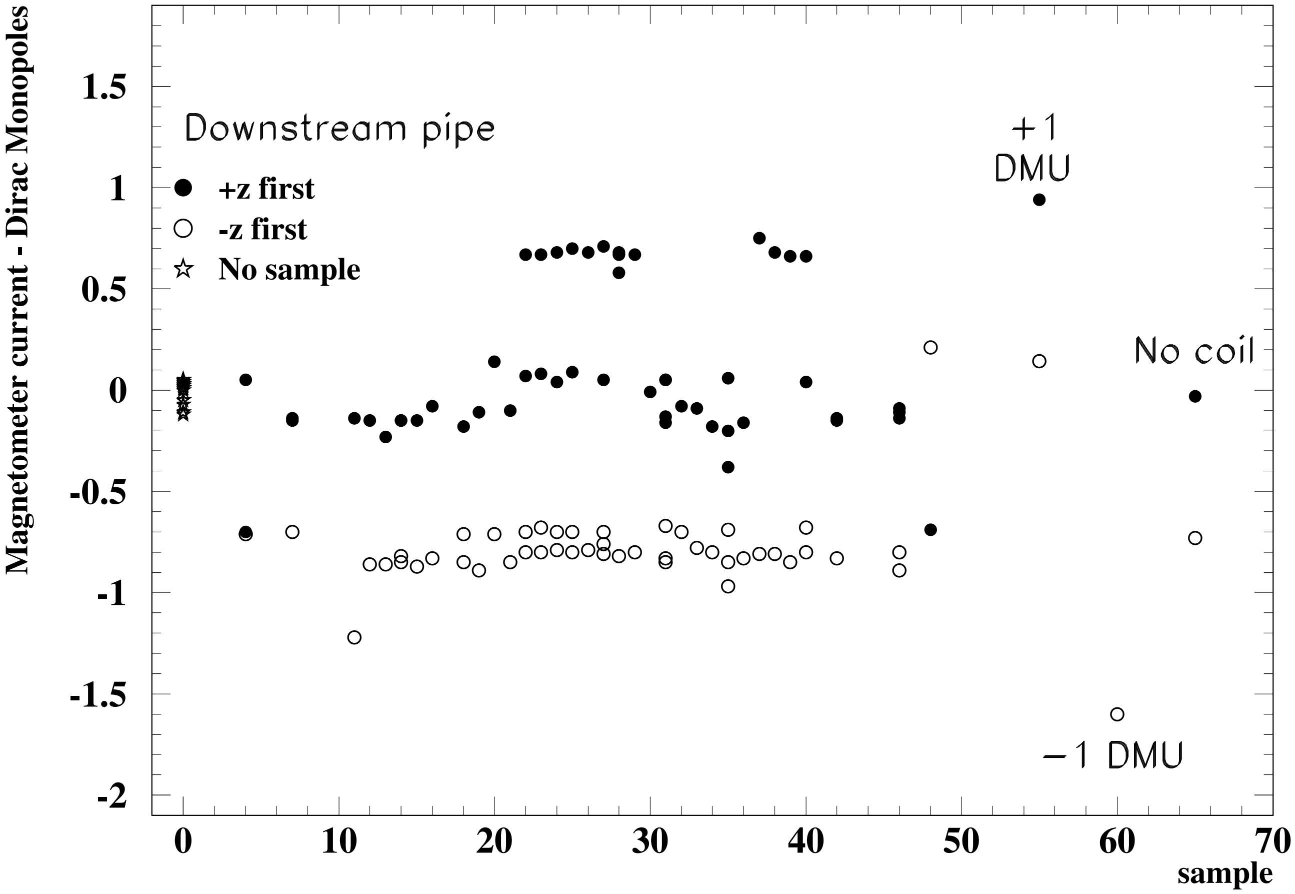

Figure 15: The data from figure 4 together with the data from samples 55, 60 and 65. These 3 samples are each from pipe 3 strips 9 and 10 paired, with the calibration coil 2 superposed. For sample 55 the coil carried a current equivalanet to +1.07 Dirac Monopoles (labelled +1 DMU). For sample 60 the coil carried a current equivalent to -1.07 Dirac Monopoles (labelled -1 DMU, the +z traversal was lost for this reading due to a large flux jump). Sample 65 is the result for the same pair of strips but without the calibration coil 2.

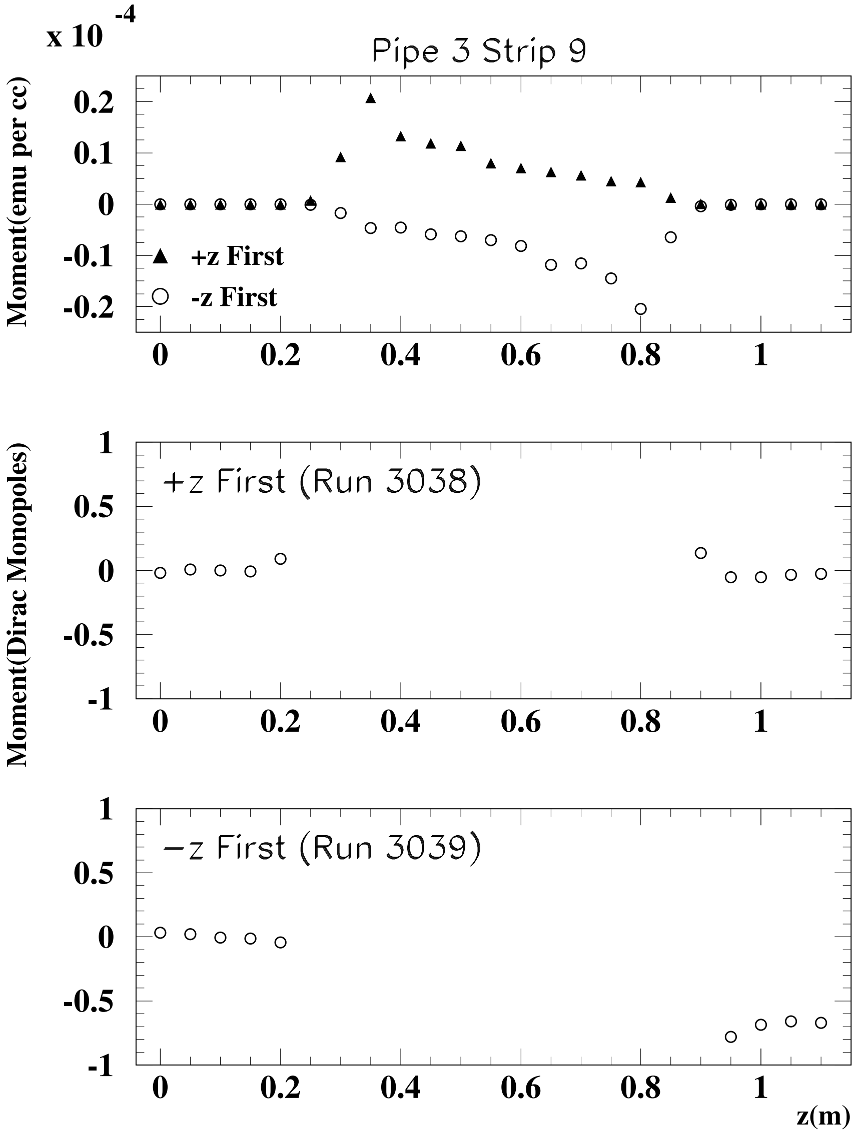

Figure 16: Upper plot shows the measured values of $Bz_{intensity}$ as a function of z as a strip (pipe 3 number 9) passes through. The middle (lower) plot shows the values of $Bz_{intensity}$ vs z on a larger scale as the strip is passed through in the +z (-z) direction. It can be seen that there is no step for the +z first traversal and a -0.7 Dirac Monopole Units for the -z first traversal i.e. the same behaviour as the May run.

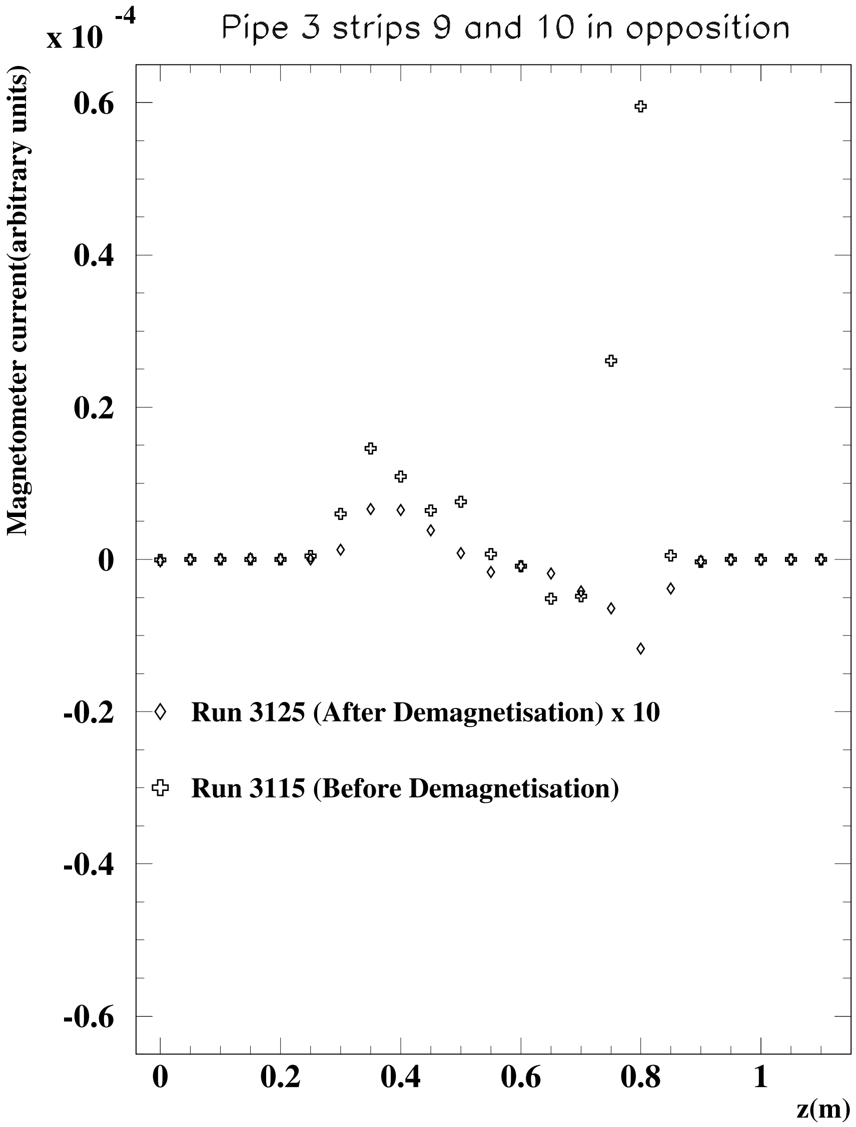

Figure 17: The relative dipole moment (approx emu per cm^3 within a factor 2) labelled magnetometer current as a function of the z position of the strip for the same strips shown in figure 11 before and after demagnetisation (times 10) at 0.1 Tesla at 400 Hz. It can be seen that demagnetisation reduces the dipole moments by a factor ~ 20.

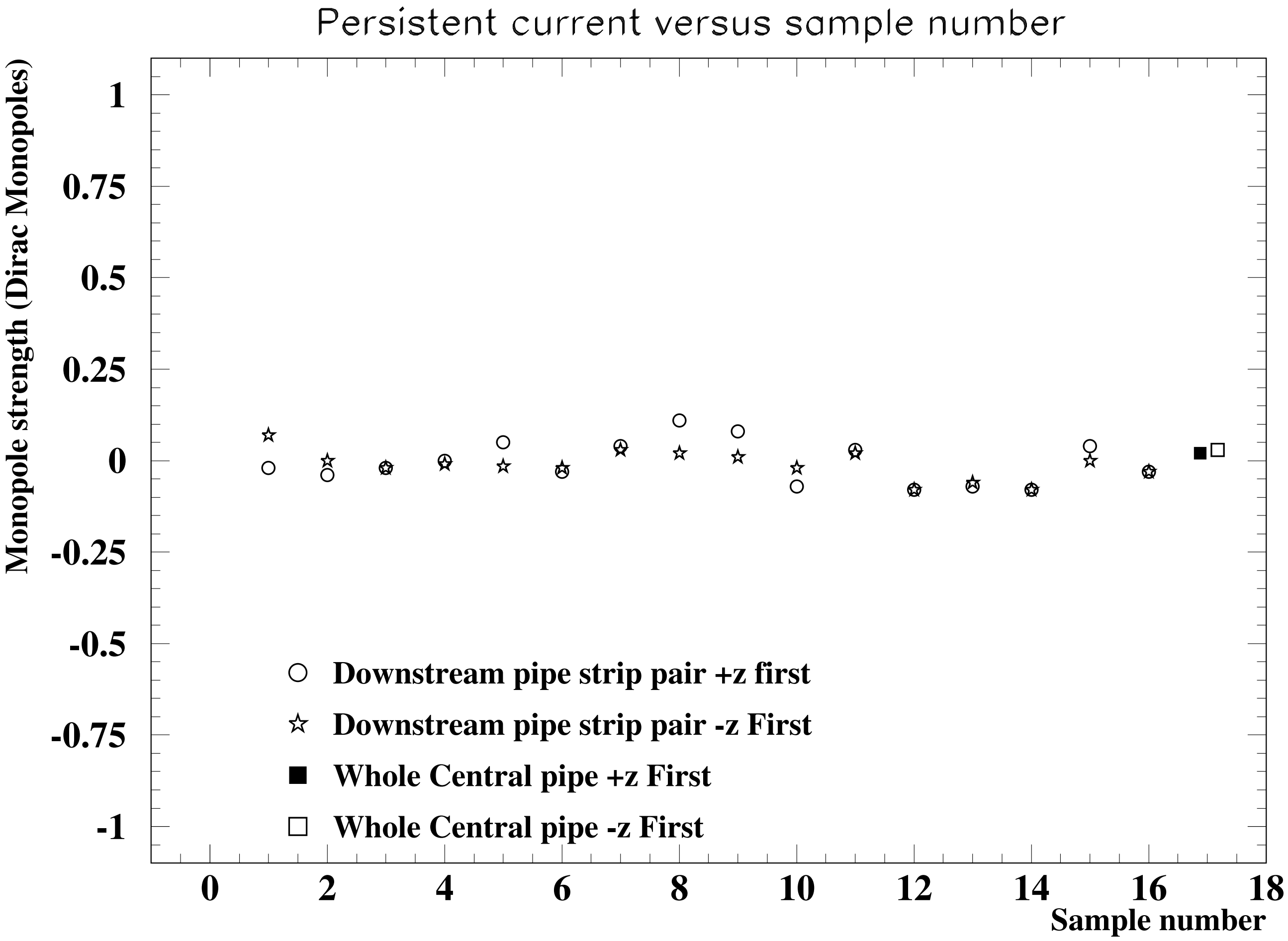

Figure 18: The results of the 15 Jan 2004 run after all sample had been demagnetised.

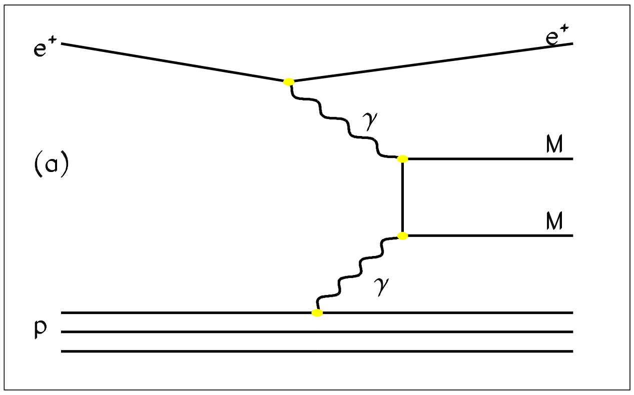

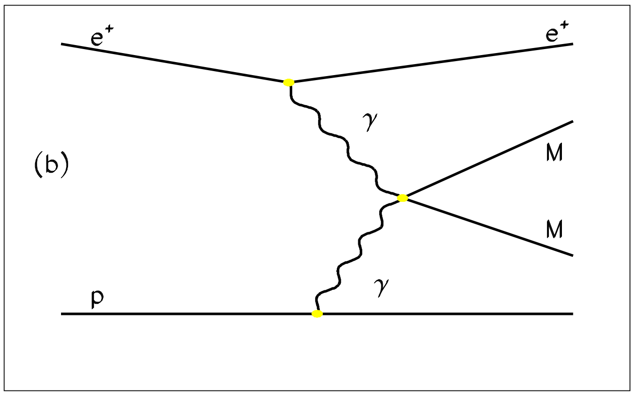

Figure 19: Feynman graphs for the two models considered, a) the gamma-gamma fusion model where the monopoles are a pair of oppositely magnetically charged spin 1/2 fermions b) the gamma-gamma contact interaction producing a pair of oppositely magnetically charged bosons of spin 1.

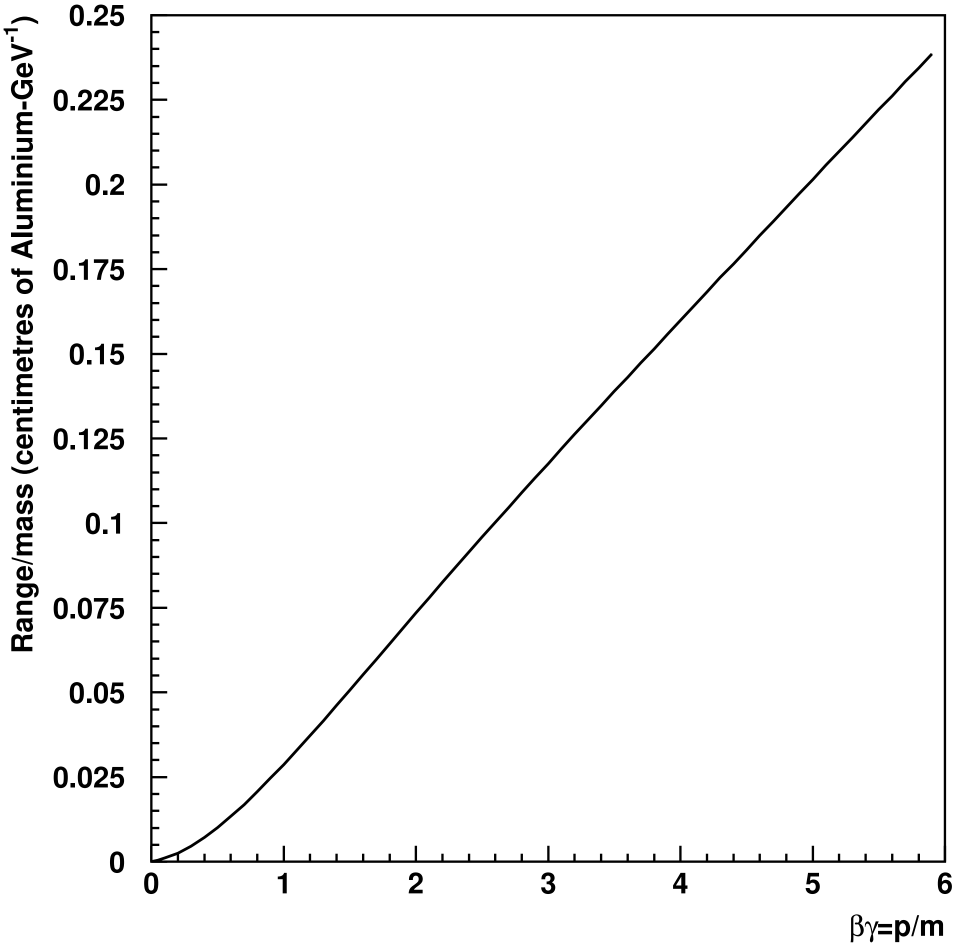

Figure 20: Range/Mass of a monopole of strength 1 Dirac Monopole Unit as a function of $p/m = \beta\gamma$ in aluminium. The range decreases as the square of the magnetic charge.

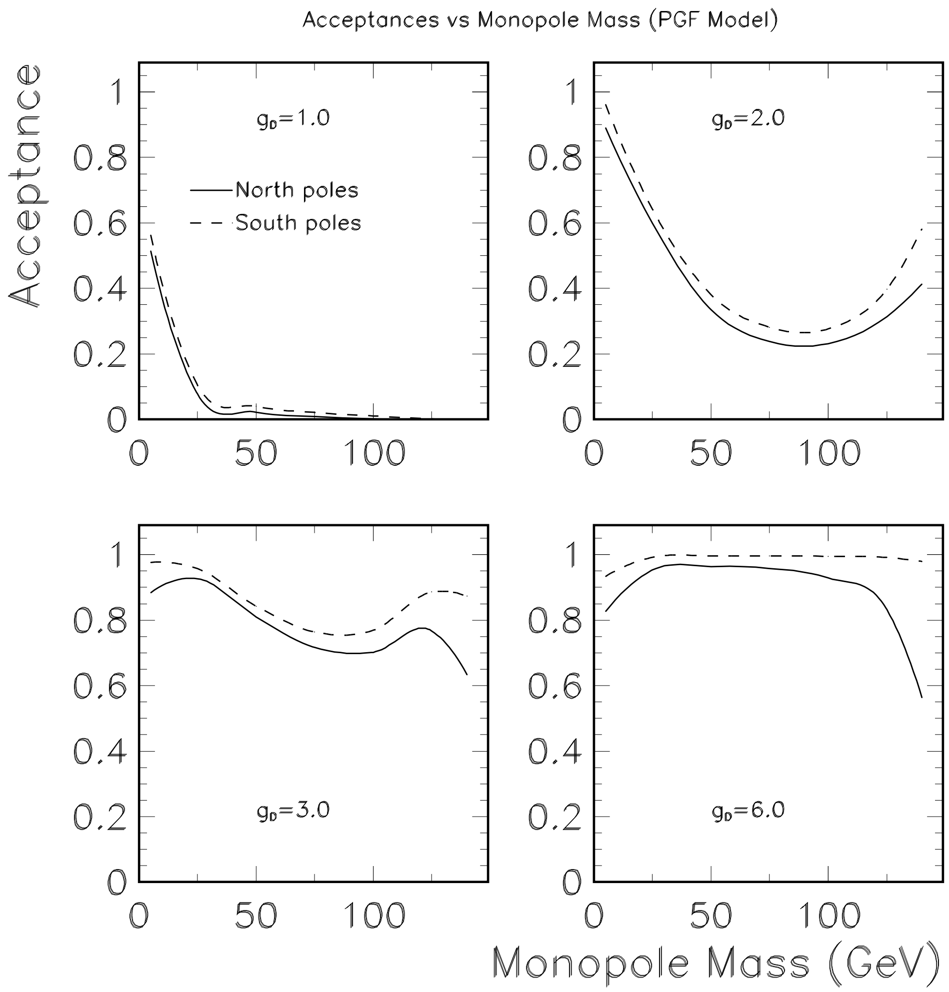

Figure 21: Acceptance as a function of monopole mass as computed from the photon-photon fusion model for different magnetic charges. The monopoles are assumed to be spin 1/2 fermions in this model.

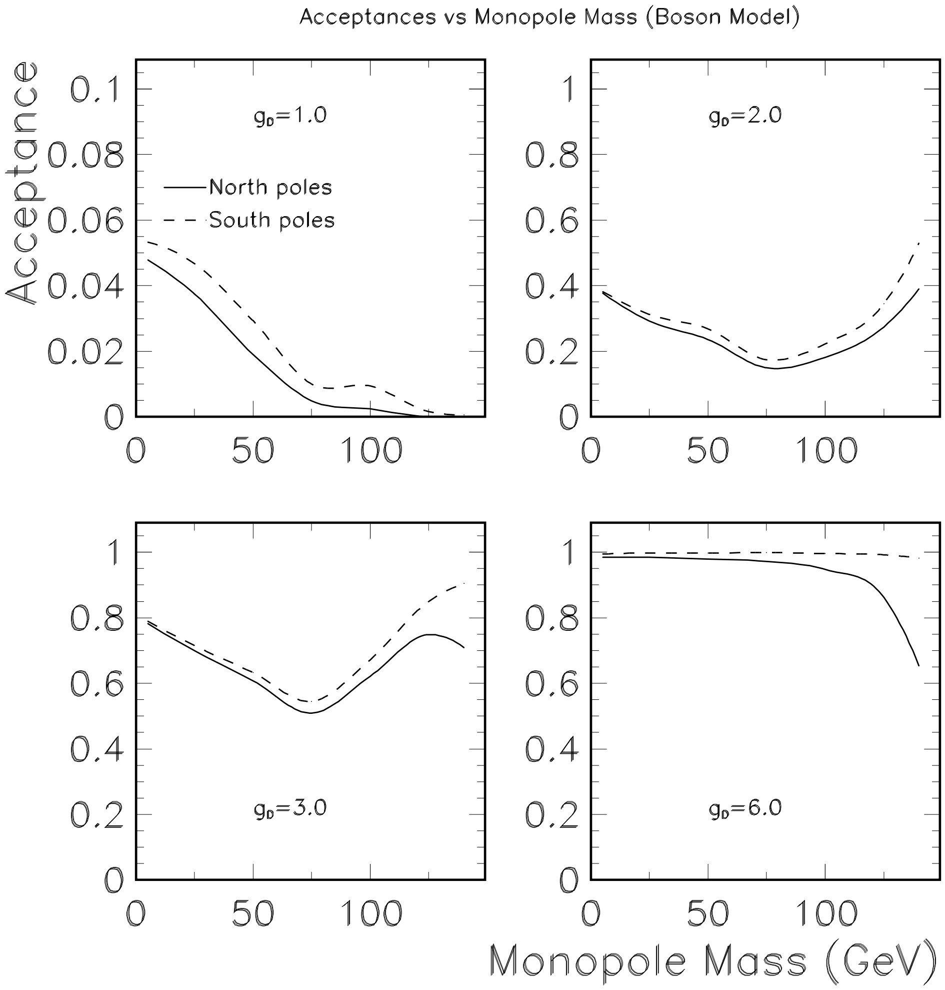

Figure 22: Acceptance as a function of monopole mass as computed from the contact interaction model for different magnetic charges. The monopoles are assumed to be spin zero bosons in this model.

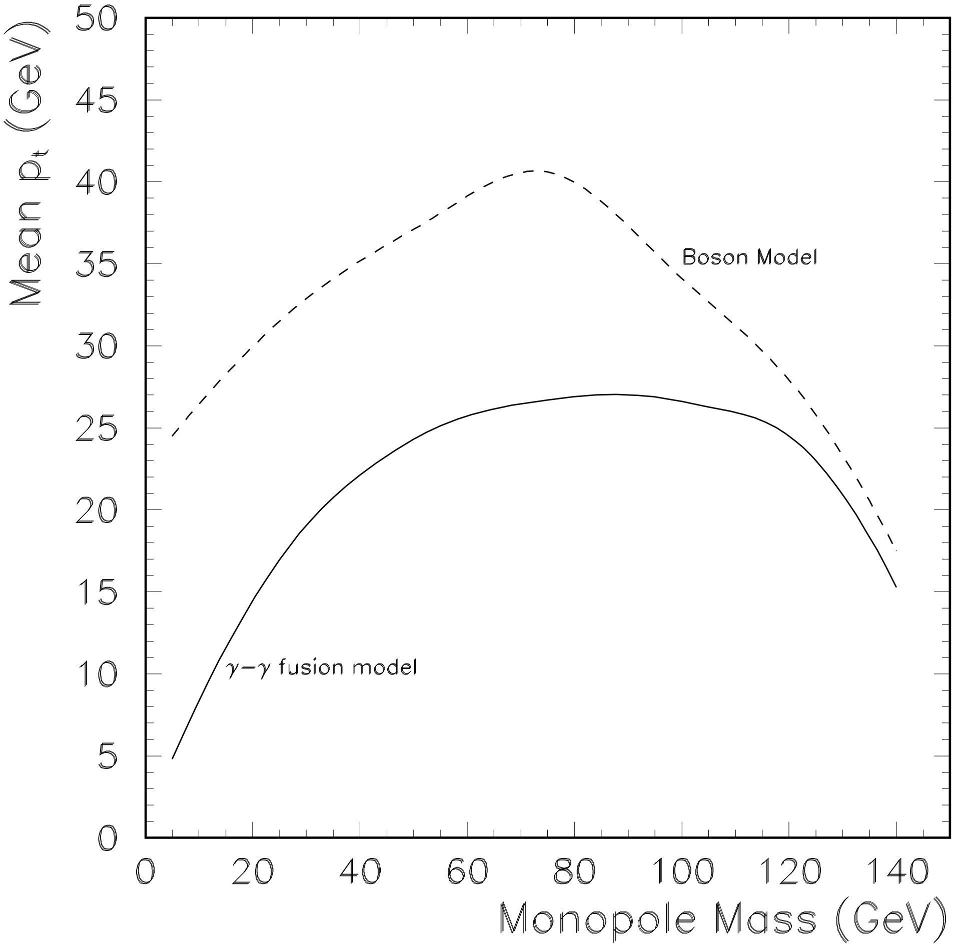

Figure 23: Average transverse mometa of monopole versus monopole mass. The dashed curve is for the contact interaction model and the solid curve for the $\gamma - \gamma$ fusion model.

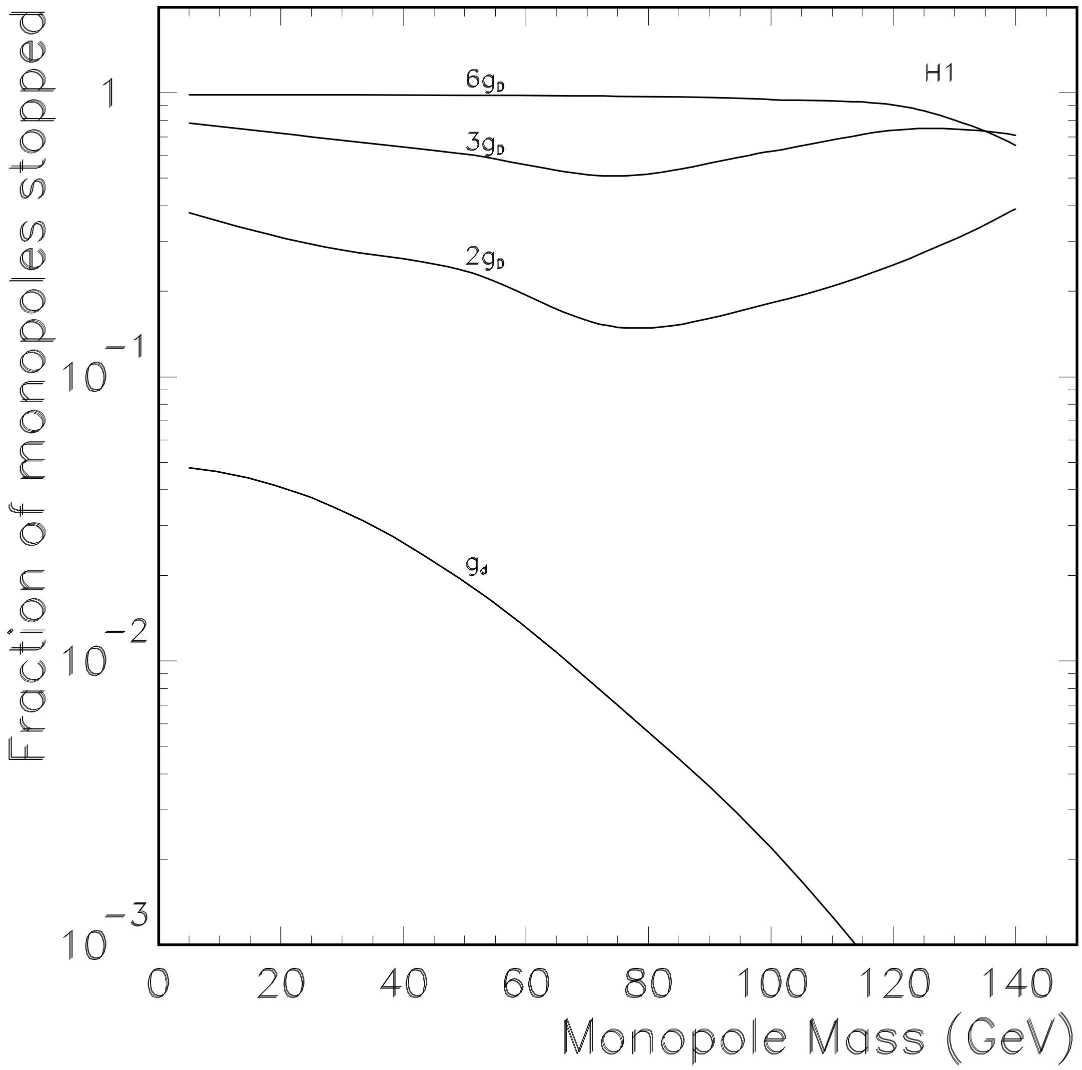

Figure 24: The acceptance assumed for monopole production as a function of monopole mass. The most conservative i.e. lowest acceptance is used i.e. that for N poles from the contact interaction model.

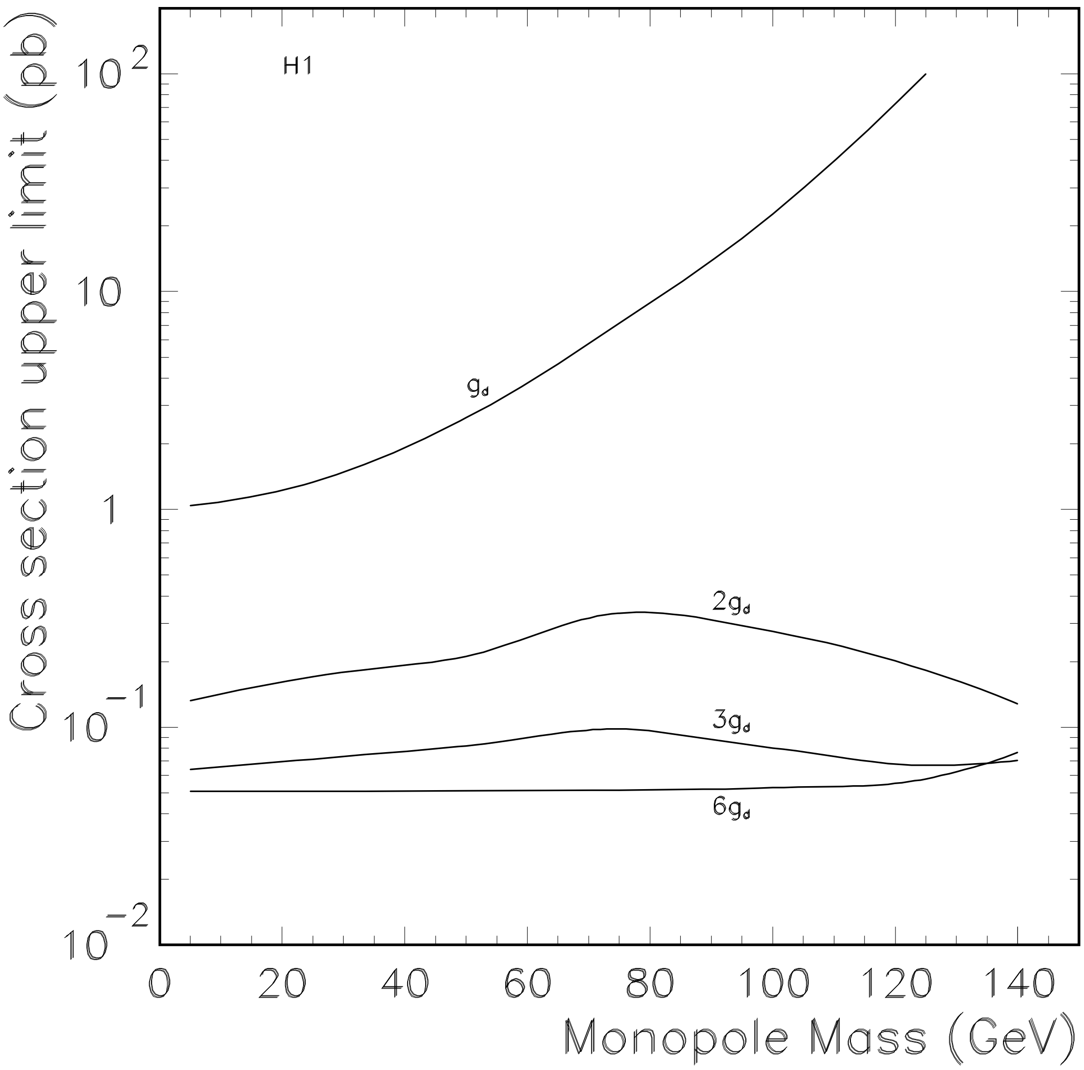

Figure 25: The upper limit at 95% confidence level on the electroproduction cross section for monopoles as a function of monopole mass. The different curves are the limits for different magnetic charges in units of the Dirac Monopole (g_d).

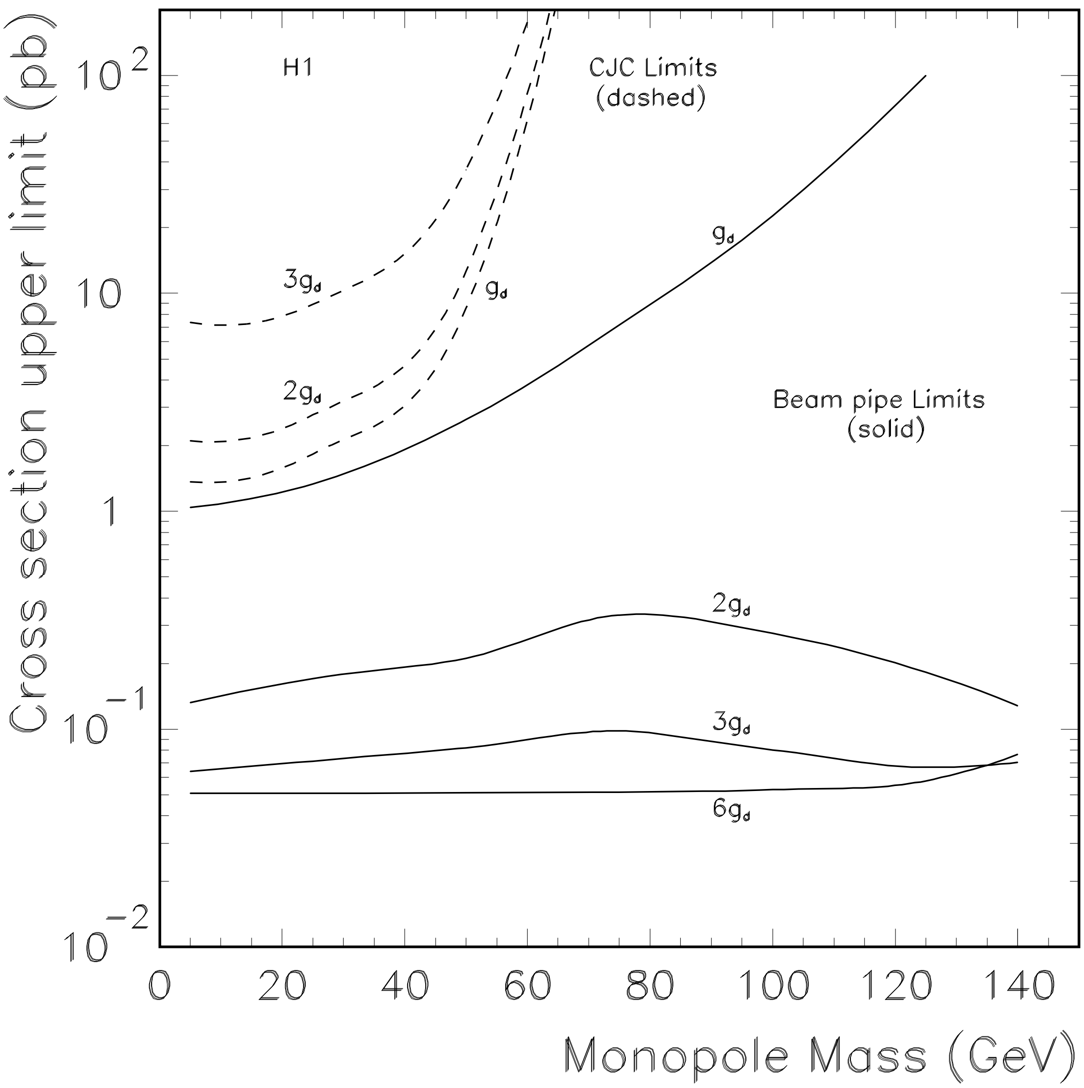

Figure 26: The upper limit at 95% confidence level on the electroproduction cross section for monopoles as a function of monopole mass. The different curves are the limits for different magnetic charges in units of the Dirac Monopole (g_d). The dashed curves show the limits from the search in the 5.53 pb^{-1} luminosity minimum bias data reported in [5]. The solid curves show the limits from the beam pipe search from figure 25.